IEEE Access
Multidisciplinary ⋮ Rapid Review ⋮ Open Access Journal

Received 26 August 2023, accepted 12 September 2023, date of publication 15 September 2023,
date of current version 27 September 2023.

*Digital Object Identifier 10.1109/ACCESS.2023.3316026*

RESEARCH ARTICLE

# Distributed Adaptive Neural Anti-Disturbance Cooperative Control of High-Order MIMO Nonlinear Multi-Agent Systems

**FEIYU JIN, LONGSHENG CHEN, WEIZHEN SUN, AND YUXIANG WANG**
School of Aircraft Engineering, Nanchang Hangkong University, Nanchang 330063, China

Corresponding author: Longsheng Chen (lschen2008@163.com)

This work was supported by the Jiangxi Provincial Natural Science Foundation under Grant 20224BAB202027 and Grant 20232ACB202007.

**ABSTRACT** In this paper, a distributed cooperative control problem for a class of high-order multi-input and multi-output (MIMO) nonlinear multiagent systems (MASs) in the presence of uncertain nonlinearities and external disturbances is addressed. A coupled design is developed to collaboratively approximate unknown nonlinearities and compounded disturbances by combining neural networks (NNs) with high-order disturbance observers (HODOs). To further simplify the controller structure, relationships among the Laplace matrix, adjacency matrix and consensus tracking errors are analyzed based on undirected communication graphs. Then, a distributed adaptive NN anti-disturbance control protocol is proposed for high-order MIMO nonlinear MASs based on the outputs of NNs and HODOs, where dynamic surface control (DSC) is introduced to eliminate the ''computational explosion'' problem of the conventional backstepping method. The semiglobally uniformly ultimate boundedness of closed-loop system signals is proven through Lyapunov theory. Finally, simulations of a quadrotor UAV formation are performed to demonstrate the effectiveness of the proposed control scheme.

**INDEX TERMS** High-order MIMO nonlinear system, multi-agent system, neural network, high-order disturbance observer, distributed cooperative control.

## I. INTRODUCTION

Multiagent systems (MASs) have been widely applied to civil and military fields due to their high efficiency, strong reliability, flexibility and fault tolerance [1], [2], [3], [4], [5], [6], [7]. A fundamental requirement of MASs is that agents need to communicate, cooperate and coordinate with each other to ensure the successful completion of tasks. Nevertheless, interactions and cooperative relationships among agents may lead to instability and performance degradation. Therefore, cooperative control design plays an important role in MASs. The most common MASs cooperative control problems include the formation problem [8], [9], cluster problem [10], and consensus problem [11], [12], [13], [14]. The consensus problem involves all agents aiming to obtain a common final state via local exchange of information; this problem has received significant attention from scholars [15], [16]. In [17], a reduced-order control protocol was developed to guarantee the coordination of continuous MASs by adopting a multistep algorithm. A distributed linear consensus protocol with second-order dynamics was first designed in [18], and more studies on the cooperative control of MASs based on consensus protocols can be found in [19] and [20]. Although the above studies have achieved positive outcomes, the design process and structure of the controller can be further simplified to make it more practical.

On the other hand, it is worth noting that all of the abovementioned approaches require the agent dynamics to be linear. However, nonlinear systems are more suitable for describing practical application scenarios than linear systems [21], [22], [23], [24]. In addition, there are difficulties in accurately modeling agents, and the uncertainties in the model could affect the performance of the system. Unfortunately, the dynamics of uncertain nonlinear MASs are difficult to ascertain, which means that a new control method must be sought beyond the traditional adaptive control

The associate editor coordinating the review of this manuscript and approving it for publication was Xiwang Dong.

method. Fortunately, neural networks (NNs) have provided some insight into the adaptive control problem for nonlinear MASs. In [25], a fully distributed NN-based adaptive control method was constructed for MASs with unmodeled dynamics. The NN was used to approximate unknown functions in the agent dynamics. This approach effectively guaranteed that all of the followers were asymptotically synchronized to the leader. Then, the method was extended to cope with consensus problems of nonlinear MASs with time-varying asymmetric state constraints, which more faithfully model real engineering systems [26]. Other NN-based approaches have been investigated in the literature [27], [28], [29], [30], [31]. Moreover, uncertainty arises from not only the system's internal factors but also external environmental disturbances. The approximation ability of NNs is effective within compact sets, whereas the range of uncertainty in reality is difficult to ascertain. Fortunately, disturbance observers (DOs) have been proven to be effective for addressing uncertainties and unknown external disturbances of systems [32], [33], [34], [35], [36]. In [32], a control method was designed to deduce mismatched uncertainties based on a nonlinear disturbance observer (NDO). To make NDOs more applicable to real-world engineering problems, a two-stage design method was proposed that separates the design of the NDO from the design of the controller to improve the disturbance attenuation ability of the nonlinear controller in [33]. However, the aforementioned DOs have a first-order form, and actual disturbances and their models are unknown. Therefore, it is necessary to consider the influences of higher-order disturbances on the system [37]. For this reason, a high-order disturbance observer (HODO) was proposed in [38]. In general, the HODO introduces more disturbance prior information so that the performance of disturbance estimation is significantly improved compared to that of DOs [39]. Combining an HODO and sliding mode control (SMC), a novel control strategy was constructed to achieve closed-loop stability of mobile-wheeled inverted pendulum (MWIP) systems [40]. Theoretically, applying both NNs and HODO could improve the anti-disturbance performance of the system. At the same time, the problem of coupling multiple approximators arises, which provides motivation for this study.

The aforementioned literatures focus mainly on systems captured by low-order dynamics, such as first- and second-order forms, and the existing results cannot be extended to high-order agent dynamics in a straightforward manner. In fact, many systems are modeled by high-order dynamics in practical engineering. For example, the single-link flexible joint manipulator system and jerk system are fourth- and third-order dynamical models [41], respectively. For high-order systems, the backstepping method formalizes and clarifies the controller design process by dividing the higher-order system into numerous lower-order subsystems. An adaptive fuzzy output feedback control method for a class of multi-input and multi-output (MIMO) nonlinear systems with immeasurable states was constructed via the backstepping technique in [42]. More information about the backstepping method is provided in [43], [44], [45], and [46]. However, the traditional backstepping method causes the "computational explosion" problem when analyzing the high-order derivatives of the virtual control law. Dynamic surface control (DSC) was proposed to solve this problem by using a first-order filter to estimate the virtual control law and the derivative at each step [47], [48], [49], [50]. In [47], the principles and technical details of DSC are elaborated upon, and they are further developed and applied in [48], [49], and [50]. However, to the best of our knowledge, cooperative control of MIMO nonlinear MASs with high-order dynamics has received little attention. In fact, it is not a trivial work to design appropriate controllers for high-order MIMO nonlinear MASs due to their complexity and generality, that is, any of the above systems can be regarded as a special case of high-order MIMO nonlinear MASs.

Motivated by the above observations and analysis, a distributed adaptive neural anti-disturbance cooperative control protocol for a class of high-order MIMO nonlinear MASs is developed. To address nonlinear uncertainties and external disturbances, NNs and HODOs are applied for controller design. Furthermore, DSC technology is used to reduce the burden of "computational explosion". The main contributions of this note are as follows:

1) Combining the advantages of the NNs and HODO techniques, the effects of uncertain nonlinearities and external disturbances on MASs are addressed, and in addition, the problem of coupling multiple approximators is also addressed in this paper.

2) Compared to the cooperative control method designed in [36], the design process and structure of the controller are further simplified in this paper by exploiting the relationships among the Laplace matrix, adjacency matrix and consensus tracking errors. On this basis, the introduction of DSC technology additionally reduces the computational burden.

3) Compared with the existing results on distributed cooperative control of high-order SISO MASs or first- and second-order MASs [20], [24], the results of this paper, which account for both high-order nonlinear dynamics and MIMO properties, are more general and thus cover a broader class of applications. It is shown that the semiglobally uniform ultimate boundedness (SGUUB) of closed-loop system signals and asymptotic consensus of all agent outputs hold.

The rest of this paper is organized as follows. Section II introduces basic graph theory and describes the problem. Section III provides the design procedure of the constructed distributed cooperative controller and proof of stability. The simulation experiment and discussion are presented in Section IV. This paper ends with a conclusion in Section V.

*Notation:* $\|\bullet\|$ represents the Frobenius norm for a matrix or the Euclidean norm for a vector. Let $\mathbf{1}_m$ and $I_m$ denote, respectively, the $m \times 1$ column vector of all ones and the

$m \times m$ identity matrix. $\hat{D}_{il}^{q(\ell)}$ denotes the $l^{th}$ disturbance estimate for the $q^{th}$ subsystem of the $i^{th}$ agent; the superscript $\ell$ means the $\ell^{th}$ order derivative of $\hat{D}_i^q$. For a matrix $\boldsymbol{A}$, $\lambda_{\max}(A)$ and $\lambda_{\min}(A)$ denote the maximum and minimum eigenvalues of $\boldsymbol{A}$, respectively. $\otimes$ and $\odot$ denote the Kronecker product and the Hadamard product, respectively. To facilitate subsequent theoretical derivations and proofs, a novel notation $\odot_{\mathfrak{m}}$ is defined to combine matrix multiplication with the Hadamard product. The details are as follows: Let $\mathfrak{A} = [\mathfrak{a}_1, \mathfrak{a}_2, \cdots, \mathfrak{a}_{\mathfrak{m}}]^{\mathrm{T}}$, $\mathfrak{a}_{\mathfrak{l}} = [\mathfrak{a}_{\mathfrak{l}1}, \mathfrak{a}_{\mathfrak{l}2}, \cdots, \mathfrak{a}_{\mathfrak{l}\mathfrak{n}}]^{\mathrm{T}}$, $\mathfrak{B} = [\mathfrak{b}_1, \mathfrak{b}_2, \cdots, \mathfrak{b}_{\mathfrak{m}}]^{\mathrm{T}}$, $\mathfrak{b}_{\mathfrak{l}} = [\mathfrak{b}_{\mathfrak{l}1}, \mathfrak{b}_{\mathfrak{l}2}, \cdots, \mathfrak{b}_{\mathfrak{l}\mathfrak{n}}]^{\mathrm{T}}$, $\mathfrak{l} = 1, 2, \cdots, \mathfrak{m}$; then, $\mathfrak{A} \otimes_{\mathfrak{m}} \mathfrak{B} = [\mathfrak{a}_1^{\mathrm{T}} \mathfrak{b}_1, \mathfrak{a}_2^{\mathrm{T}} \mathfrak{b}_2, \cdots, \mathfrak{a}_{\mathfrak{m}}^{\mathrm{T}} \mathfrak{b}_{\mathfrak{m}}]^{\mathrm{T}}$.

## II. PRELIMINARIES AND PROBLEM STATEMENT

### A. ALGEBRAIC GRAPH THEORY

The communication topology among $N(N \geqslant 2)$ agents can be described by undirected graphs and directed graphs. Assuming that each node corresponds to an agent, the topology of $N$ nodes is represented by an undirected graph $\mathcal{G} = (\mathcal{V}, \mathcal{E}, \mathcal{A})$, where $\mathcal{V} = (1, 2, \cdots, N)$ is a nonempty set of nodes, $\mathcal{E} = \{(i, j),\ i, j \in \mathcal{V}\}$ is the set of edges formed by ordered edges of all nodes, and $\mathcal{A} = \left[a_{ij}\right] \in R^{N \times N}$ is the weighted adjacency matrix. If $(i, j) \in \mathcal{E}$, then node $i$ and node $j$ can communicate with each other and $a_{ij} > 0$; otherwise, $a_{ij} = 0$. If $\mathcal{G}$ has no loops, then $a_{ii} = 0$. Define $b_i = \sum_j^N a_{ij}, j \neq i$, as the weighted in-degree of node $i$ and $\mathcal{B} = diag\{b_1, b_2, \cdots, b_N\} \in R^{N \times N}$ as the in-degree matrix. Then, the Laplacian matrix is defined by $L = \mathcal{B} - \mathcal{A}$. Assuming that there is a virtual leader among the MASs, $H = diag\{h_1, h_2, \cdots, h_N\}$, is defined as the leader-follower adjacency matrix, and $h_i$ is the contact weight between agent $i$ and the virtual leader. When agent $i$ and the virtual leader can communicate, $h_i > 0$; otherwise, $h_i = 0$.

### B. PROBLEM STATEMENT

Consider a class of high-order MIMO nonlinear MASs in the presence of uncertainties and external disturbances. The system of agent $i$ is given as follows:

$$\begin{aligned} \dot{x}_i^q &= F_i^q(\bar{x}_i^q) + G_i^q(\bar{x}_i^q)x_i^{q+1} + \Delta f_i^q(\bar{x}_i^q) + d_i^q(\bar{x}_i^q, t), \\ &\qquad q = 1, 2, \cdots, n-1, \\ \dot{x}_i^n &= F_i^n(\bar{x}_i^n) + G_i^n(\bar{x}_i^n)u_i + \Delta f_i^n(\bar{x}_i^n) + d_i^n(\bar{x}_i^n, t), \\ y_i &= x_i^1, \end{aligned} \tag{1}$$

where $i = 1, 2, \cdots, N$, $\bar{x}_i^q = [x_i^1, x_i^2, \cdots, x_i^q]^{\mathrm{T}}$, $x_i^q = [x_{i1}^q, x_{i2}^q, \cdots, x_{im}^q]^{\mathrm{T}}$ is the state vector, $u_i \in R^{\mathfrak{s}}$ and $y_i = x_i^1 \in R^m$ denote the control input and output of system (1), respectively. $F_i^q(\bar{x}_i^q) \in R^m$, $G_i^q(\bar{x}_i^q) \in R^{m \times m}$ and $G_i^n(\bar{x}_i^n) \in R^{m \times \mathfrak{s}}$ are known smooth nonlinear functions. $\Delta f_i^q(\bar{x}_i^q)$ and $d_i^q(\bar{x}_i^q, t)$, $q = 1, 2, \cdots, n$ denote the uncertainties and external time-varying disturbances of system (1), respectively.

*Remark 1:* Compared with the existing results on distributed cooperative control of high-order SISO MASs or first- and second-order MASs, the results for the considered MASs (1), which include both high-order nonlinear dynamics and MIMO properties, are more general and thus imply that the presented control strategy is more applicable to practical engineering.

The objective is to develop a distributed cooperative control protocol for the high-order MIMO nonlinear MAS (1), which can guarantee that the each agent's output signal $y_i$ in the MASs can track the virtual leader output signal $y^d$ with consensus errors converging to the neighborhood of zero, and all signals in closed-loop system are SGUUB [51].

To facilitate the control design and the stability analysis for the high-order MIMO nonlinear MAS (1), the following assumptions and lemmas are given.

*Assumption 1 [23]:* For the high-order MIMO nonlinear MAS (1), the virtual leader output signal $y^d$, its $1^{st}$ derivative $\dot{y}^d$ and $2^{nd}$ derivative $\ddot{y}^d$ are bounded; that is, there exists an unknown constant $B_0 > 0$ such that $\Pi_0 = \{(y^d,\ \dot{y}^d,\ \ddot{y}^d) : \left\|y^d\right\|^2 + \left\|\dot{y}^d\right\|^2 + \left\|\ddot{y}^d\right\|^2 \leqslant B_0\}$.

*Assumption 2:* For the high-order MIMO nonlinear MAS (1), the unknown external time-varying disturbances $d_i^q$ and its $r^{th}$ derivative are bounded, that is, there exists unknown constant $\beta_i^{q\ell} > 0$ such that $\left\|d_i^{q(\ell)}\right\| < \beta_i^{q\ell}$, where $\ell = 0, 1, \cdots, r$ and $q = 1, 2, \cdots, n$.

*Assumption 3:* For the high-order MIMO nonlinear MAS (1), the inverse matrix of $G_i^q \in R^{m \times m}$ exists, $q = 1, 2, \cdots, n-1$, and the generalized inverse matrix of $G_i^n \in R^{m \times \mathfrak{s}}$ exists. In addition, there exists a positive constant $\bar{\lambda}_i^q$ such that $\lambda_{\max}(G_i^q G_i^{q\mathrm{T}}) \leqslant \bar{\lambda}_i^q$, $q = 1, 2, \cdots, n$.

*Lemma 1 [49]:* Consider a nonlinear control system $\dot{x} = f(x, u)$ with state $x \in R^m$, control input $u \in R^{\mathfrak{s}}$ and bounded initial conditions, if there exists a Lyapunov function $V(x)$ satisfying $\boldsymbol{\omega}_1(\|x\|) \leqslant V(x) \leqslant \boldsymbol{\omega}_2(\|x\|)$ such that $\dot{V}(x) \leqslant -\kappa V(x) + M$, where $\boldsymbol{\omega}_1, \boldsymbol{\omega}_2$: $R^m \to R$ are class $K$ functions, $\kappa$ and $M$ are positive constants, then the system state $x(t)$ is SGUUB.

*Lemma 2 [31]:* The continuous function $f(\mathbf{Z}) : R^{\iota} \to R$ is approximated by using RBFNNs as follows:

$$\hat{f}(\mathbf{Z}) = \hat{W}^{\mathrm{T}}\Phi(\mathbf{Z}) + \boldsymbol{\tau} \tag{2}$$

where $\boldsymbol{Z} = [\mathrm{Z}_1,\ \mathrm{Z}_2,\ \cdots,\ \mathrm{Z}_{\iota}]^{\mathrm{T}}$ is the input vector of the neural network, $\hat{W} = [\hat{W}_1, \hat{W}_2, \cdots, \hat{W}_{\iota}]^{\mathrm{T}}$ is the weight vector of the neural network, $\Phi(\mathbf{Z}) = [\Phi_1(\mathbf{Z}),\ \Phi_2(\mathbf{Z}), \cdots, \Phi_{\iota}(\mathbf{Z})\ ]^{\mathrm{T}}$ is the vector of radial basis functions, and $\boldsymbol{\tau}$ is an approximation error with bound.

The optimal weight vector $W^*$ is denoted as:

$$W^* = \arg \min_{\hat{W} \in \Omega_f} [\sup_{Z \in S_Z} |\hat{f}(\mathbf{Z}|\hat{W}) - f(\mathbf{Z})] \tag{3}$$

where $\Omega_f = \left\{\hat{W} : \left\|\hat{W}\right\| \leqslant \bar{M}\right\}$ is the feasible region of the estimated parameters, $\bar{M}$ is the design parameter, and $S_Z$ is the feasible region of the state vector.

Using the maximum weight, the following formula is obtained:

$$f(\mathbf{Z}) = W^{*\mathrm{T}}\Phi(\mathbf{Z}) + \boldsymbol{\tau}^* \tag{4}$$

where $|\boldsymbol{\tau}^*| \leqslant \bar{\boldsymbol{\tau}}$ is the optimal approximation error and $\bar{\boldsymbol{\tau}}$ is the upper bound on the approximation error. In this study, the Gaussian RBF is employed: $\Phi(\mathbf{Z}) = \exp\left(-(\mathbf{Z}-\boldsymbol{\sigma})^{\mathrm{T}}(\mathbf{Z}-\boldsymbol{\sigma})/\mu^2\right)$, in which $\boldsymbol{\sigma}$ and $\mu$ denote the center and width of the NN, respectively.

*Lemma 3 [52]:* Let $\mathbb{X}$ and $\mathbb{Y}$ be two matrices or vectors of compatible dimensions. For a positive constant $\mathfrak{b}$, the following inequality is true:

$$\mathbb{X}^{\mathrm{T}}\mathbb{Y} + \mathbb{Y}^{\mathrm{T}}\mathbb{X} \leqslant \mathfrak{b}\mathbb{X}^{\mathrm{T}}\mathbb{X} + \mathfrak{b}^{-1}\mathbb{Y}^{\mathrm{T}}\mathbb{Y} \tag{5}$$

## III. DISTRIBUTED ADAPTIVE NN ANTI-DISTURBANCE COOPERATIVE CONTROL

In this section, an RBFNN-based HODO is designed to handle uncertainties and unknown time-varying disturbances, and a distributed cooperative control strategy is developed for the high-order MIMO nonlinear MAS (1) based on the outputs of RBFNN and HODO. A schematic diagram of the distributed adaptive NN anti-disturbance cooperative control scheme is shown in Fig. 1.

### A. DESIGN OF HODO BASED ON RBFNN

First, an RBFNN is used to approximate $\Delta f_i^q$, which is the uncertainty term of the $q^{th}$ subsystem of the $i^{th}$ agent. Using optimal weights, the uncertainty can be expressed as follows:

$$\begin{aligned}\Delta f_i^q &= (\boldsymbol{\Gamma}_i^q)^{-1}[W_i^{q*}\odot_m \boldsymbol{\Phi}_i^q(Z_i^q) + \boldsymbol{\tau}_i^{q*}]\\ &= (\boldsymbol{\Gamma}_i^q)^{-1}W_i^{q*}\odot_m \boldsymbol{\Phi}_i^q(Z_i^q) + (\boldsymbol{\Gamma}_i^q)^{-1}\boldsymbol{\tau}_i^{q*}\end{aligned} \tag{6}$$

where $\boldsymbol{\Gamma}_i^q = diag(\Gamma_{i1}^q, \Gamma_{i2}^q, \cdots, \Gamma_{im}^q) > 0$ is the design parameter matrix, $W_i^{q*} = [W_{i1}^{q*}, W_{i2}^{q*}, \cdots, W_{im}^{q*}]^{\mathrm{T}}$ is the optimal weight matrix of the $q^{th}$ subsystem of the $i^{th}$ agent, $W_{il}^{q*} = [W_{il1}^{q*}, W_{il2}^{q*}, \cdots, W_{il\iota}^{q*}]^{\mathrm{T}}$, $l = 1, 2, \cdots, m$ and $\iota$ represent the number of rules, and $\bar{\boldsymbol{\Phi}}_i^q(Z_i^q) = [\Phi_{i1}^q(Z_i^q), \Phi_{i2}^q(Z_i^q), \cdots, \Phi_{i\iota}^q(Z_i^q)]^{\mathrm{T}}$ is the vector of radial basis functions. Let $\boldsymbol{\Phi}_i^q(Z_i^q) = \mathbf{1}_m \otimes \bar{\boldsymbol{\Phi}}_i^q(Z_i^q)$. By the definition of the symbol $\odot_m$, $W_i^{q*}\odot_m\boldsymbol{\Phi}_i^q = [W_{i1}^{q*\mathrm{T}}\bar{\boldsymbol{\Phi}}_i^q, W_{i2}^{q*\mathrm{T}}\bar{\boldsymbol{\Phi}}_i^q, \cdots, W_{im}^{q*\mathrm{T}}\bar{\boldsymbol{\Phi}}_i^q]^{\mathrm{T}}$, and $\boldsymbol{\tau}_i^{q*}$ is the approximation error of the $i^{th}$ agent and satisfies $\|\boldsymbol{\tau}_i^{q*}\| \leqslant \bar{\boldsymbol{\tau}}_i^q$.

Then, the unknown compounded disturbance of the subsystem of system (1) is defined as follows:

$$D_i^q = (\boldsymbol{\Gamma}_i^q)^{-1}\boldsymbol{\tau}_i^{q*} + d_i^q \tag{7}$$

The compounded disturbance consists of the approximation error of the NN and the external time-varying disturbance. According to Assumption 2 and Lemma 2, $\dot{D}_i^q$ is bounded; that is, there exists $\bar{D}_i^q$ such that $\|\dot{D}_i^q\| \leqslant \bar{D}_i^q$.

Based on (6) and (7), system (1) can be rewritten as

$$\begin{aligned}\dot{x}_i^q &= F_i^q(\bar{x}_i^q) + G_i^q(\bar{x}_i^q)x_i^{q+1} + (\boldsymbol{\Gamma}_i^q)^{-1}(W_i^{q*}\odot_m\boldsymbol{\Phi}_i^q) + D_i^q,\\ &\quad q = 1, 2, \cdots, n-1,\\ \dot{x}_i^n &= F_i^n(\bar{x}_i^n) + G_i^n(\bar{x}_i^n)u_i + (\boldsymbol{\Gamma}_i^n)^{-1}(W_i^{n*}\odot_m\boldsymbol{\Phi}_i^n) + D_i^n,\\ y_i &= x_i^1,\end{aligned} \tag{8}$$

Since the compounded disturbance $D_i^q$ cannot be measured directly, the $r^{th}$ order HODO for system (8) is proposed as follows:

$$\hat{D}_i^{q(\ell-1)} = \boldsymbol{\eta}_i^{q\ell} + k_i^{q\ell}x_i^q \tag{9}$$

$$\begin{aligned}\dot{\boldsymbol{\eta}}_i^{q\ell} &= -k_i^{q\ell}\Big(F_i^q + G_i^q x_i^{q+1} + (\boldsymbol{\Gamma}_i^q)^{-1}(\hat{W}_i^q\odot_m\boldsymbol{\Phi}_i^q)\\ &\quad + \hat{D}_i^q\Big) + \hat{D}_i^{q(\ell-1)}, \ell = 1, 2, \cdots, r-1\end{aligned} \tag{10}$$

and

$$\hat{D}_i^{q(r-1)} = \boldsymbol{\eta}_i^{qr} + k_i^{qr}x_i^q \tag{11}$$

$$\dot{\boldsymbol{\eta}}_i^{qr} = -k_i^{qr}\left(F_i^q + G_i^q x_i^{q+1} + (\boldsymbol{\Gamma}_i^q)^{-1}(\hat{W}_i^q\odot_m\boldsymbol{\Phi}_i^q) + \hat{D}_i^q\right) \tag{12}$$

where

$$k_i^{q\ell} = \begin{bmatrix} k_{i11}^{q\ell} & k_{i12}^{q\ell} & \cdots & k_{i1m}^{q\ell}\\ k_{i21}^{q\ell} & k_{i22}^{q\ell} & \cdots & k_{i2m}^{q\ell}\\ \vdots & \vdots & \ddots & \vdots\\ k_{ir1}^{q\ell} & k_{ir2}^{q\ell} & \cdots & k_{imm}^{q\ell}\end{bmatrix}, \quad \ell = 1, 2, \cdots, r \tag{13}$$

is a constant matrix that is selected by the designer. $\hat{D}_i^{q(\ell-1)}$ is estimate value of $D_i^{q(\ell-1)}$, and $\boldsymbol{\eta}_i^{q\ell} \in R^m$ is auxiliary variable. Define the estimation error of the HODO as $\tilde{D}_i^{q(\ell-1)} = D_i^{q(\ell-1)} - \hat{D}_i^{q(\ell-1)}$, $\ell = 1, 2, \cdots, r$. $\hat{W}_i$ is the estimate of $W_i^*$, and $\tilde{W}_i = W_i^* - \hat{W}_i$ denotes the estimation error.

Invoking (8) and differentiating (9) and (11) yields

$$\begin{aligned}\frac{d\tilde{D}_i^q}{dt} &= \frac{dD_i^q}{dt} - \frac{d\hat{D}_i^q}{dt} = \frac{dD_i^q}{dt} - \frac{d(\boldsymbol{\eta}_{i1}^q + k_{i1}^q x_i^q)}{dt}\\ &= \tilde{D}_i^{q(1)} - k_i^{q1}(\boldsymbol{\Gamma}_i^q)^{-1}(\tilde{W}_i^q\odot_m\boldsymbol{\Phi}_i^q) - k_i^{q1}\tilde{D}_i^q\\ \frac{d\tilde{D}_i^{q(1)}}{dt} &= \frac{d\dot{D}_i^q}{dt} - \frac{d\dot{\hat{D}}_i^q}{dt}\\ &= \tilde{D}_i^{q(2)} - k_i^{q2}(\boldsymbol{\Gamma}_i^q)^{-1}(\tilde{W}_i^q\odot_m\boldsymbol{\Phi}_i^q) - k_i^{q2}\tilde{D}_i^q\\ \frac{d\tilde{D}_i^{q(r-1)}}{dt} &= \frac{dD_i^{q(r-1)}}{dt} - \frac{d\hat{D}_i^{q(r-1)}}{dt}\\ &= \tilde{D}_i^{q(r)} - k_i^{qr}(\boldsymbol{\Gamma}_i^q)^{-1}(\tilde{W}_i^q\odot_m\boldsymbol{\Phi}_i^q) - k_i^{qr}\tilde{D}_i^q.\end{aligned}$$

Define $\tilde{\boldsymbol{\mathcal{D}}}_i^q = [\tilde{D}_i^q, \tilde{D}_i^{q(1)}, \cdots, \tilde{D}_i^{q(r-1)}]^{\mathrm{T}}$. The observer error dynamics can be written as

$$\dot{\tilde{\boldsymbol{\mathcal{D}}}}_i^q = K_i^q\tilde{\boldsymbol{\mathcal{D}}}_i^q + \boldsymbol{\mathcal{D}}_i^{q*} + K_i^{q*}\otimes\left((\boldsymbol{\Gamma}_i^q)^{-1}(\tilde{W}_i^q\odot_m\boldsymbol{\Phi}_i^q)\right) \tag{14}$$

where

$$K_i^q = \begin{bmatrix} -k_i^{q1} & I_m & \cdots & 0 & 0\\ -k_i^{q2} & 0 & I_m & \cdots & 0\\ \vdots & \vdots & \vdots & \vdots & \vdots\\ -k_i^{qr} & 0 & 0 & \cdots & 0\end{bmatrix}$$

$$\boldsymbol{\mathcal{D}}_i^{q*} = \begin{bmatrix} 0\\ 0\\ \vdots\\ D_i^{q(r)}\end{bmatrix}, \quad K_i^{q*} = \begin{bmatrix} -k_i^{q1}\\ -k_i^{q2}\\ \vdots\\ -k_i^{qr}\end{bmatrix}$$

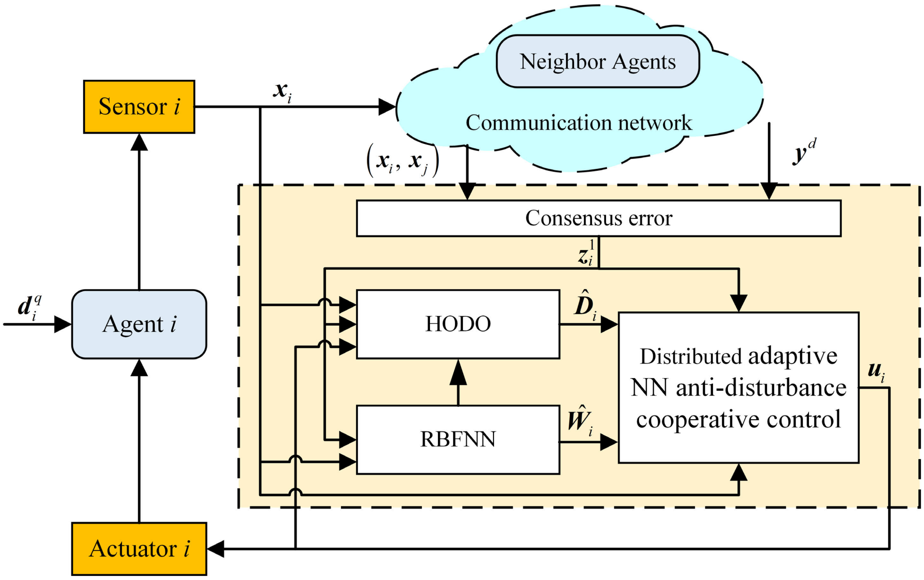

**FIGURE 1.** Schematic diagram of the distributed adaptive NN anti-disturbance cooperative control.

and $I_m \in R^{m\times m}$ is the identity matrix. Since $K_i^q$ is a Hurwitz matrix, for a specified matrix $Q_i^q = Q_i^{q\mathrm{T}} > 0$, there exists a positive symmetric matrix $P_i^q$ such that

$$K_i^{q\mathrm{T}} P_i^q + P_i^q K_i^q = -Q \tag{15}$$

*Remark 2:* In this work, an HODO is employed to estimate the compounded disturbances. Earlier work on DOs often assumed that the disturbance was bounded and its derivative decayed to or even equaled zero [32]. In the case of the HODO, this assumption was relaxed to Assumption 2 and comparatively practical. Furthermore, the HODO allow high tracking accuracy to be obtained by estimating the disturbance and its $(r-1)^{th}$ order derivatives.

### B. DISTRIBUTED COOPERATIVE ANTI-DISTURBANCE CONTROL DESIGN

In this subsection, a distributed anti-disturbance cooperative control protocol is proposed based on DSC technique. From the coordinate transformation designed by the standard backstepping approach and the definition of consensus error of an MASs, the following consensus tracking error and coordinate transformation are defined for the high-order MIMO nonlinear MAS (1):

$$z_i^1 = \sum_{j\in N} a_{ij}(x_i^1 - x_j^1) + h_i(x_i^1 - y^d) \tag{16}$$

$$z_i^q = x_i^q - \bar{\boldsymbol{\alpha}}_i^{q-1} \tag{17}$$

$$z_i^n = x_i^n - \bar{\boldsymbol{\alpha}}_i^{n-1} \tag{18}$$

where $\bar{\boldsymbol{\alpha}}_i^{q-1}$ is the output of the following first-order filter:

$$\boldsymbol{\Upsilon}_i^q \dot{\bar{\boldsymbol{\alpha}}}_i^q + \bar{\boldsymbol{\alpha}}_i^q = \boldsymbol{\alpha}_i^q, \bar{\boldsymbol{\alpha}}_i^q(0) = \boldsymbol{\alpha}_i^q(0), \quad q = 2, \cdots, n-1 \tag{19}$$

where $\boldsymbol{\Upsilon}_i^q = diag\left\{\Upsilon_{i1}^q, \Upsilon_{i2}^q, \cdots, \Upsilon_{im}^q\right\}$, $\Upsilon_{il}^q > 0$ is the time constant of the filter, and $\boldsymbol{\alpha}_i^q$ is the virtual control law of the $1^{st}$ subsystem of the $1^{st}$ agent, whose specific form will be given later. The first-order filter defined in equation (19) is the idea of DSC and addresses the problem of repeatedly differentiating $\boldsymbol{\alpha}_i^q$.

To facilitate the subsequent controller design and stability analysis, the following lemma is first given.

*Lemma 4:* Define $\tilde{L} = L + H \in R^N$ and $\mathcal{L}(\bullet) = \bullet \otimes I_m$, where $\otimes$ is the Kronecker product and $I_m$ is the $m \times m$ identity matrix; then, the augmented matrix $\mathcal{L}(\tilde{L}) \in R^{Nm\times Nm}$ is positive definite and satisfies:

$$\begin{aligned}\frac{1}{2}X^{1T}\mathcal{L}(\tilde{L})X^1 &= \frac{1}{2}(Z^1 + \boldsymbol{\varpi})^T \Delta (Z^1 + \boldsymbol{\varpi}) \\ &= \frac{1}{2}(Z^1 + \boldsymbol{\varpi})^T X^1\end{aligned} \tag{20}$$

where $X^1 = [x_1^1, x_2^1, \cdots, x_N^1]^T \in R^{Nm}$, $z_i^1 = [z_{i1}^1, z_{i2}^1, \cdots, z_{im}^1]^T \in R^m$, $Z^1 = [z_1^1, z_2^1, \cdots, z_N^1]^T \in R^{Nm}$, $\varpi_i = [h_i y_1^d, h_i y_2^d, \cdots, h_i y_m^d]^T$, $\boldsymbol{\varpi} = [\varpi_1, \varpi_2, \cdots, \varpi_N]^T$, $z_{il}^1 = \sum_{j\in N} a_{ij}(x_{il}^1 - x_{jl}^1) + h_i(x_{il}^1 - y_l^d)$, and $z_{il}^1$, $x_{il}^1$ and $y_l^d$ denote the $l^{th}$ component of the consensus tracking error vector $z_i^1$, the state vector $x_i^1$ and the virtual leader output vector $y^d$, respectively.

*Proof:* From the definition of the augmented matrix $\mathcal{L}(\bullet)$, the following equation holds:

$$\mathcal{L}(\tilde{L}) = \mathcal{L}(L + H) = \mathcal{L}(L) + \mathcal{L}(H) \tag{21}$$

where $\mathcal{L}(L) \in R^{Nm\times Nm}$ and $\mathcal{L}(H) \in R^{Nm\times Nm}$ are both real symmetric matrices. Since $\mathcal{L}(H)$ is a diagonal matrix with main diagonal elements $h_i \geq 0$, $\mathcal{L}(H)$ is semipositive definite. Noting

$$\mathcal{L}(L) = \mathcal{L}(\mathcal{B} - \mathcal{A}) = \begin{pmatrix} c_{11} & \cdots & c_{1Nm} \\ \vdots & \ddots & \vdots \\ c_{Nm1} & \cdots & c_{NmNm} \end{pmatrix} \tag{22}$$

let $\lambda_0$ be any eigenvalue of $\mathcal{L}(L)$ and $\xi_0$ be the eigenvector associated with $\lambda_0$, such that $\mathcal{L}(L)\xi_0 = \lambda_0\xi_0$. The $i^{th}$ component of $\boldsymbol{\xi}_0$ is $\xi_i (i = 1, 2, \cdots, Nm)$, and $\mathcal{L}(L)\boldsymbol{\xi}_0 = \lambda_0\boldsymbol{\xi}_0$ can be expressed as a system of linear equations as follows:

$$\begin{cases} c_{11}\xi_1 + c_{12}\xi_2 + \cdots + c_{1Nm}\xi_{Nm} = \lambda_0\xi_1 \\ c_{21}\xi_1 + c_{22}\xi_2 + \cdots + c_{2Nm}\xi_{Nm} = \lambda_0\xi_2 \\ \quad\vdots \qquad\quad \vdots \qquad\qquad \vdots \qquad\qquad \vdots \\ c_{Nm1}\xi_1 + c_{Nm2}\xi_2 + \cdots + c_{NmNm}\xi_{Nm} = \lambda_0\xi_{Nm} \end{cases} \tag{23}$$

Suppose $|\xi_s|$ is the largest of magnitudes $|\xi_1|, |\xi_2|, \cdots, |\xi_{Nm}|$. Based on (23), the following formula holds:

$$\begin{aligned} &(\lambda_0 - c_{ss})\xi_s \\ &= c_{s1}\xi_1 + \cdots + c_{s(s-1)}\xi_{s-1} \\ &\quad + c_{s(s+1)}\xi_{s+1} + \cdots + c_{sNm}\xi_{Nm} \end{aligned} \tag{24}$$

$$\begin{aligned} &|(\lambda_0 - c_{ss})|\,|\xi_s| \\ &\leq |c_{s1}|\,|\xi_1| + \cdots + \left|c_{s(s-1)}\right|\,|\xi_{s-1}| + \left|c_{s(s+1)}\right|\,|\xi_{s+1}| \\ &\quad + \cdots + |c_{sNm}|\,|\xi_{Nm}| \\ &\leq \left(|c_{s1}| + \cdots + \left|c_{s(s-1)}\right| + \left|c_{s(s+1)}\right| + \cdots + |c_{sNm}|\right)|\xi_s| \end{aligned} \tag{25}$$

$$\begin{aligned} &c_{rr} - \hbar \\ &\leq \lambda_0 \leq c_{rr} + \hbar \end{aligned} \tag{26}$$

where $\hbar = |c_{s1}| + \cdots + \left|c_{s(s-1)}\right| + \left|c_{s(s+1)}\right| + \cdots + |c_{sNm}|$. From graph theory, it follows that

$$\begin{aligned} c_{ss} &= -(c_{s1} + \cdots + c_{s(s-1)} + c_{s(s+1)} + \cdots + c_{sNm}) \\ &= \hbar \geq 0 \end{aligned} \tag{27}$$

It follows from (26) and (27) that any eigenvalue of $\mathcal{L}(L)$ satisfies $\lambda_0 \geq 0$. Whereupon $\mathcal{L}(L)$ is a semipositive definite real symmetric matrix. Considering $\mathcal{L}(\tilde{L}) = \mathcal{L}(L) + \mathcal{L}(H)$, it is possible to obtain eigenvalues of $\mathcal{L}(\tilde{L})$ satisfying $\tilde{\lambda}_0 \geq 0$. $\mathcal{L}(\tilde{L})$ is a semipositive definite real symmetric matrix, whose $Nm$ eigenvalues are $\lambda_1, \lambda_2, \cdots, \lambda_{Nm}$. Define $\boldsymbol{\xi} = (\xi_1, \xi_2, \cdots, \xi_{Nm}) \in R^{Nm\times Nm}$ as the orthogonal matrix of $\mathcal{L}(\tilde{L})$ and $\xi_1, \xi_2, \cdots, \xi_{Nm}$ as the eigenvectors corresponding to the eigenvalues $\lambda_1, \lambda_2, \cdots, \lambda_{Nm}$, one obtains $\boldsymbol{\xi}^T\boldsymbol{\xi} = \boldsymbol{\xi}\boldsymbol{\xi}^T = I_{Nm}$, where $I_{Nm} \in R^{Nm\times Nm}$ is the identity matrix. Then, it follows from real symmetric matrix properties that

$$\begin{aligned} \frac{1}{2}X^{1T}\mathcal{L}(\tilde{L})X^1 &= \frac{1}{2}X^{1T}\boldsymbol{\xi}^T\Lambda\boldsymbol{\xi}X^1 \\ &= \frac{1}{2}X^{1T}\boldsymbol{\xi}^T\Lambda\boldsymbol{\xi}\boldsymbol{\xi}^T\Lambda^{-1}\boldsymbol{\xi}\boldsymbol{\xi}^T\Lambda\boldsymbol{\xi}X^1 \\ &= \frac{1}{2}X^{1T}\mathcal{L}(\tilde{L})\boldsymbol{\xi}^T\Lambda^{-1}\boldsymbol{\xi}\mathcal{L}(\tilde{L})X^1 \\ &= \frac{1}{2}(Z^1 + \boldsymbol{\varpi})^T\Delta(Z^1 + \boldsymbol{\varpi}) \end{aligned} \tag{28}$$

where $\Lambda = diag\,[\lambda_1, \lambda_2, \cdots, \lambda_{Nm}]$ and $\Delta = \boldsymbol{\xi}^T\Lambda^{-1}\boldsymbol{\xi}$.

Combining the Laplace matrix with the definition of the matrix $\mathcal{L}(\tilde{L})$ leads to:

$$\frac{1}{2}X^{1T}\mathcal{L}(\tilde{L})X^1 = \frac{1}{2}(Z^1 + \boldsymbol{\varpi})^T X^1 \tag{29}$$

This concludes the proof.

*Remark 3:* Lemma 4 reveals the relationships among the Laplace matrix, adjacency matrix and consensus tracking errors, which will be useful later in controller design and stability analysis.

*Step 1:* It follows from the designed HODO in (9), (10), (11) and (12) that the estimate valve of the compounded $D_i^1$ in the $1^{st}$ subsystems can be expressed as

$$\hat{D}_i^{1(\ell-1)} = \boldsymbol{\eta}_i^{1\ell} + k_i^{1\ell}x_i^1 \tag{30}$$

$$\begin{aligned} \dot{\boldsymbol{\eta}}_i^{1\ell} &= -k_i^{1\ell}\left(F_i^1 + G_i^1x_i^2 + (\boldsymbol{\Gamma}_i^1)^{-1}(\hat{W}_i^1\odot_m\boldsymbol{\Phi}_i^1) + \hat{D}_i^1\right) \\ &\quad + \hat{D}_i^{1(\ell-1)}, \ell = 1, 2, \cdots, r-1 \end{aligned} \tag{31}$$

and

$$\hat{D}_i^{1(r-1)} = \boldsymbol{\eta}_i^{1r} + k_i^{1r}x_i^1 \tag{32}$$

$$\dot{\boldsymbol{\eta}}_i^{1r} = -k_i^{1r}\left(F_i^1 + G_i^1x_i^2 + (\boldsymbol{\Gamma}_i^1)^{-1}(\hat{W}_i^1\odot_m\boldsymbol{\Phi}_i^1) + \hat{D}_i^1\right) \tag{33}$$

It follows from (14) and (16) that the observer error dynamic and consensus error of $1^{st}$ subsystem are given as follows:

$$\dot{\tilde{\boldsymbol{\mathcal{D}}}}_i^1 = K_i^1\tilde{\boldsymbol{\mathcal{D}}}_i^1 + \boldsymbol{\mathcal{D}}_i^{1*} + K_i^{1*} \otimes \left((\boldsymbol{\Gamma}_i^1)^{-1}(\tilde{W}_i^1\odot_m\boldsymbol{\Phi}_i^1)\right) \tag{34}$$

$$z_i^1 = \sum_{j\in N} a_{ij}(x_i^1 - x_j^1) + h_i(x_i^1 - y^r) \tag{35}$$

Then, the virtual control law and updating law are designed as follows:

$$\begin{aligned} \boldsymbol{\alpha}_i^1 = (-G_i^1)^{-1}\Big[&C_i^1(z_i^1 + \boldsymbol{\varpi}_i) + F_i^1 + \\ &(\boldsymbol{\Gamma}_i^1)^{-1}(\hat{W}_i^1\odot_m\boldsymbol{\Phi}_i^1) + \hat{D}_i^1\Big] \end{aligned} \tag{36}$$

$$\dot{\hat{W}}_i^1 = (\boldsymbol{\Gamma}_i^1)^{-1}[\boldsymbol{\Phi}_i^1 \odot (z_i^1 + \boldsymbol{\varpi}_i) - \lambda_i^1\hat{W}_i^1] \tag{37}$$

where the matrix $C_i^1$ is chosen to satisfy $\lambda_{\min}(C_i^1) \geqslant \frac{k_i}{2}\lambda_{\max}(\Delta) + \frac{1}{2}(\bar{\lambda}_i^1 + 1)$, $k_i > 0$, $C_i^1 = (C_i^1)^{\mathrm{T}} > 0$ and $\boldsymbol{\Gamma}_i^1 = \boldsymbol{\Gamma}_i^{1\mathrm{T}} > 0$ are designed parameters.

*Remark 4:* Because the relationships among the Laplace matrix, adjacency matrix and consensus tracking errors have been analyzed, compared with the previous design in [36], the proposed first-order virtual control law exhibits a relatively simple structure, which facilitates the subsequent controller design and stability proof.

*Step 2:* It follows from the equation (17) that the tracking error of the $2^{nd}$ subsystem of the $i^{th}$ agent can be defined as follows:

$$z_i^2 = x_i^2 - \bar{\boldsymbol{\alpha}}_i^1 \tag{38}$$

where $\bar{\boldsymbol{\alpha}}_i^1$ is the filtered signal of the virtual control signal $\boldsymbol{\alpha}_i^1$ designed in the $1^{st}$ step, and taking the derivative of both sides of equation (38) with respect to time yields

$$\begin{aligned} \dot{z}_i^2 = F_i^2(\bar{x}_i^2) + G_i^2(\bar{x}_i^2)x_i^3 + (\boldsymbol{\Gamma}_i^2)^{-1}(W_i^{2*}\odot_m\boldsymbol{\Phi}_i^2) \\ + D_i^2 - \dot{\bar{\boldsymbol{\alpha}}}_i^1 \end{aligned} \tag{39}$$

Similar to step 1, an HODO is constructed to approximate the compounded disturbance $D_i^2$ as follows:

$$\hat{D}_i^{2(\ell-1)} = \boldsymbol{\eta}_i^{2\ell} + k_i^{2\ell} x_i^2 \tag{40}$$

$$\dot{\boldsymbol{\eta}}_i^{2\ell} = -k_i^{2\ell}\left(F_i^2 + G_i^2 x_i^3 + (\boldsymbol{\Gamma}_i^2)^{-1}(\hat{W}_i^2 \odot_m \boldsymbol{\Phi}_i^2) + \hat{D}_i^2\right) + \hat{D}_i^{2(\ell-1)}, \quad \ell = 1, 2, \cdots, r-1 \tag{41}$$

and

$$\hat{D}_i^{2(r-1)} = \boldsymbol{\eta}_i^{2r} + k_i^{2r} x_i^2 \tag{42}$$

$$\dot{\boldsymbol{\eta}}_i^{2r} = -k_i^{2r}\left(F_i^2 + G_i^2 x_i^3 + (\boldsymbol{\Gamma}_i^2)^{-1}(\hat{W}_i^2 \odot_m \boldsymbol{\Phi}_i^2) + \hat{D}_i^2\right) \tag{43}$$

It follows from (14) and (16) that the observer error dynamic and consensus error of 2nd subsystem are given as follows:

$$\dot{\tilde{\boldsymbol{\mathcal{D}}}}_i^2 = K_i^2 \tilde{\boldsymbol{\mathcal{D}}}_i^2 + \boldsymbol{\mathcal{D}}_i^{2*} + K_i^{2*} \otimes \left((\boldsymbol{\Gamma}_i^2)^{-1}(\tilde{W}_i^2 \odot_m \boldsymbol{\Phi}_i^2)\right) \tag{44}$$

Then, the virtual control signal $\boldsymbol{\alpha}_i^2$ and updating law are constructed as follows:

$$\boldsymbol{\alpha}_i^2 = (-G_i^2)^{-1}\Big[C_i^2 z_i^2 + G_i^{1\mathrm{T}}(z_i^1 + \boldsymbol{\varpi}_i) + F_i^2 + (\boldsymbol{\Gamma}_i^2)^{-1}(\hat{W}_i^2 \odot_m \boldsymbol{\Phi}_i^2) + \hat{D}_i^2\Big] \tag{45}$$

$$\dot{\hat{W}}_i^2 = (\boldsymbol{\Gamma}_i^2)^{-1}[\boldsymbol{\Phi}_i^2 \odot z_i^2 - \lambda_i^2 \hat{W}_i^2] \tag{46}$$

where $C_i^2 = (C_i^2)^{\mathrm{T}} > 0$ and $\boldsymbol{\Gamma}_i^2 = (\boldsymbol{\Gamma}_i^2)^{\mathrm{T}} > 0$ are designed parameters.

*Step q (3 $\leqslant$ q $\leqslant$ n - 1):* Similarly, it follows from equation (17) that the tracking error of the $q^{th}$ subsystem of the $i^{th}$ agent can be defined as follows:

$$z_i^q = x_i^q - \bar{\boldsymbol{\alpha}}_i^{q-1} \tag{47}$$

where $\bar{\boldsymbol{\alpha}}_i^{q-1}$ is the filtered signal of the virtual control signal $\boldsymbol{\alpha}_i^{q-1}$ designed in the $q^{th}$ step, and taking the derivative of both sides of equation (38) with respect to time yields

$$\dot{z}_i^q = F_i^q(\bar{x}_i^q) + G_i^q(\bar{x}_i^q)x_i^{q+1} + (\boldsymbol{\Gamma}_i^q)^{-1}(W_i^{q*} \odot_m \boldsymbol{\Phi}_i^q) + D_i^q - \dot{\bar{\boldsymbol{\alpha}}}_i^{q-1} \tag{48}$$

Similar to step 1, an HODO is constructed to approximate the compounded disturbance $D_i^q$ as follows:

$$\hat{D}_i^{q(\ell-1)} = \boldsymbol{\eta}_i^{q\ell} + k_i^{q\ell} x_i^q \tag{49}$$

$$\dot{\boldsymbol{\eta}}_i^{q\ell} = -k_i^{q\ell}\left(F_i^q + G_i^q x_i^{q+1} + (\boldsymbol{\Gamma}_i^q)^{-1}(\hat{W}_i^q \odot_m \boldsymbol{\Phi}_i^q) + \hat{D}_i^q\right) + \hat{D}_i^{q(\ell-1)}, \quad \ell = 1, 2, \cdots, r-1 \tag{50}$$

and

$$\hat{D}_i^{q(r-1)} = \boldsymbol{\eta}_i^{qr} + k_i^{qr} x_i^q \tag{51}$$

$$\dot{\boldsymbol{\eta}}_i^{qr} = -k_i^{qr}\left(F_i^q + G_i^q x_i^{q+1} + (\boldsymbol{\Gamma}_i^q)^{-1}(\hat{W}_i^q \odot_m \boldsymbol{\Phi}_i^q) + \hat{D}_i^q\right) \tag{52}$$

Then, the observer error dynamic of the $q^{th}$ step can be expressed as follows:

$$\dot{\tilde{\boldsymbol{\mathcal{D}}}}_i^q = K_i^q \tilde{\boldsymbol{\mathcal{D}}}_i^q + \boldsymbol{\mathcal{D}}_i^{q*} + K_i^{q*} \otimes \left((\boldsymbol{\Gamma}_i^q)^{-1}(\tilde{W}_i^q \odot_m \boldsymbol{\Phi}_i^q)\right) \tag{53}$$

The virtual control signal $\boldsymbol{\alpha}_i^q$ and updating law are constructed as follows:

$$\boldsymbol{\alpha}_i^q = (-G_i^q)^{-1}\Big[C_i^q z_i^q + G_i^{q-1\mathrm{T}} z_i^{q-1} + F_i^q + (\boldsymbol{\Gamma}_i^q)^{-1}(\hat{W}_i^q \odot_m \boldsymbol{\Phi}_i^q) + \hat{D}_i^q\Big] \tag{54}$$

$$\dot{\hat{W}}_i^q = (\boldsymbol{\Gamma}_i^q)^{-1}[\boldsymbol{\Phi}_i^q \odot z_i^q - \lambda_i^q \hat{W}_i^q] \tag{55}$$

where $C_i^q = (C_i^q)^{\mathrm{T}} > 0$ and $\boldsymbol{\Gamma}_i^q = (\boldsymbol{\Gamma}_i^q)^{\mathrm{T}} > 0$ are designed parameters.

*Step n:* It follows from the equation (18) that the tracking error of the $n^{th}$ subsystem of the $i^{th}$ agent can be defined as follows:

$$z_i^n = x_i^n - \bar{\boldsymbol{\alpha}}_i^{n-1} \tag{56}$$

where $\bar{\boldsymbol{\alpha}}_i^{n-1}$ is the filtered signal of the virtual control signal $\boldsymbol{\alpha}_i^{n-1}$ designed in the $n^{th}$ step, and taking the derivative of both sides of equation (56) with respect to time yields

$$\dot{z}_i^n = F_i^n(\bar{x}_i^n) + G_i^n(\bar{x}_i^n)u_i + (\boldsymbol{\Gamma}_i^n)^{-1}(W_i^{n*} \odot_m \boldsymbol{\Phi}_i^n) + D_i^n - \dot{\bar{\boldsymbol{\alpha}}}_i^{n-1} \tag{57}$$

Similar to step 1, an HODO is constructed to approximate the compounded disturbance $D_i^n$ as follows:

$$\hat{D}_i^{n(\ell-1)} = \boldsymbol{\eta}_i^{n\ell} + k_i^{n\ell} x_i^n \tag{58}$$

$$\dot{\boldsymbol{\eta}}_i^{n\ell} = -k_i^{n\ell}\left(F_i^n + G_i^n u_i + (\boldsymbol{\Gamma}_i^n)^{-1}(\hat{W}_i^n \odot_m \boldsymbol{\Phi}_i^n) + \hat{D}_i^n\right) + \hat{D}_i^{n(\ell-1)}, \quad \ell = 1, 2, \cdots, r-1 \tag{59}$$

and

$$\hat{D}_i^{n(r-1)} = \boldsymbol{\eta}_i^{nr} + k_i^{nr} x_i^n \tag{60}$$

$$\dot{\boldsymbol{\eta}}_i^{nr} = -k_i^{nr}\left(F_i^n + G_i^n u_i + (\boldsymbol{\Gamma}_i^n)^{-1}(\hat{W}_i^n \odot_m \boldsymbol{\Phi}_i^n) + \hat{D}_i^n\right) \tag{61}$$

Then, the observer error dynamic of the $n^{th}$ step is given as follows:

$$\dot{\tilde{\boldsymbol{\mathcal{D}}}}_i^n = K_i^n \tilde{\boldsymbol{\mathcal{D}}}_i^n + \boldsymbol{\mathcal{D}}_i^{n*} + K_i^{n*} \otimes \left((\boldsymbol{\Gamma}_i^n)^{-1}(\tilde{W}_i^n \odot_m \boldsymbol{\Phi}_i^n)\right) \tag{62}$$

The desired actual control signal $u_i$ and updating law are constructed as follows:

$$u_i = -G_i^n(G_i^n G_i^{n\mathrm{T}})^{-1}\Big[C_i^n z_i^n + G_i^{n-1\mathrm{T}} z_i^{n-1} + F_i^n + (\boldsymbol{\Gamma}_i^n)^{-1}(\hat{W}_i^n \odot_m \boldsymbol{\Phi}_i^n) - \dot{\bar{\boldsymbol{\alpha}}}_i^{n-1} + \hat{D}_i^n\Big] \tag{63}$$

$$\dot{\hat{W}}_i^n = (\boldsymbol{\Gamma}_i^n)^{-1}[\boldsymbol{\Phi}_i^n \odot z_i^n - \lambda_i^n \hat{W}_i^n] \tag{64}$$

where $C_i^n = (C_i^n)^{\mathrm{T}} > 0$ and $\boldsymbol{\Gamma}_i^n = (\boldsymbol{\Gamma}_i^n)^{\mathrm{T}} > 0$ are the designed parameters.

*Theorem 1:* Consider the high-order MIMO nonlinear MAS (1) in the presence of uncertainties and external disturbances satisfying Assumptions 1-4, if the distributed adaptive NN anti-disturbance cooperative control protocol (63) with the HODO and updating laws shown in (30)-(33), (40)-(43), (49)-(52), (58)-(61), (37), (46), (55) and (64) is applied to the high-order MIMO nonlinear MAS, the following results can be guaranteed:

(1) All the signals of the closed-loop system are SGUUB.

(2) The output $y_i$ of each agent in the MAS can track the virtual leader output signal $y^d$ with consensus errors converging to the neighborhood of zero.

*Proof:* Define the filtering error of a first-order filter as

$$\boldsymbol{\varepsilon}_i^q = \bar{\boldsymbol{\alpha}}_i^q - \boldsymbol{\alpha}_i^q, \qquad q = 1, 2, \cdots, n-1 \tag{65}$$

Differentiating both sides of equation (65) with respect to time $t$ yields

$$\begin{aligned}\dot{\boldsymbol{\varepsilon}}_i^q &= -(\boldsymbol{\Upsilon}_i^q)^{-1}\boldsymbol{\varepsilon}_i^q + (-\frac{\partial \boldsymbol{\alpha}_i^q}{\partial x_i^q}\dot{x}_i^q - \frac{\partial \boldsymbol{\alpha}_i^q}{\partial z_i^q}\dot{z}_i^q \\ &\quad - \frac{\partial \boldsymbol{\alpha}_i^q}{\partial \boldsymbol{\eta}_i^q}\dot{\boldsymbol{\eta}}_i^q + \ddot{y}^d) \\ &= -(\boldsymbol{\Upsilon}_i^q)^{-1}\boldsymbol{\varepsilon}_i^q + B_i^q(\dot{z}_i^q, z_i^{q+1}, \boldsymbol{\varepsilon}_i^q, \boldsymbol{\eta}_i^q, y^d, \dot{y}^d, \ddot{y}^d)\end{aligned} \tag{66}$$

where $B_i^q(\bullet)$ is a continuous function with respect to the variables $(\dot{z}_i^q, z_i^{q+1}, \boldsymbol{\varepsilon}_i^q, \boldsymbol{\eta}_i^q, y^d, \dot{y}^d, \ddot{y}^d)$. Since the sets $\Pi_0 \in R^{3m}$ and $\Pi_1 \in R^{2m+1}$ are compact, $\Pi_0 \times \Pi_1$ is also compact. Thus, the maximum value $\bar{B}_i^q$ of function $B_i^q(\bullet)$ exists on $\Pi_0 \times \Pi_1$. Therefore,

$$\dot{\boldsymbol{\varepsilon}}_i^q \leqslant -(\boldsymbol{\Upsilon}_i^q)^{-1}\boldsymbol{\varepsilon}_i^q + \bar{B}_i^q \tag{67}$$

The candidate Lyapunov function is chosen as

$$\begin{aligned}V = \frac{1}{2}X^{1T}\mathcal{L}(\tilde{L})X^1 + \sum_{i=1}^{N}\Bigg(\sum_{q=2}^{n}\frac{1}{2}z_i^{qT}z_i^q + \sum_{q=1}^{n-1}\frac{1}{2}\boldsymbol{\varepsilon}_i^{qT}\boldsymbol{\varepsilon}_i^q \\ + \sum_{q=1}^{n}\frac{1}{2}\tilde{W}_i^{qT}\tilde{W}_i^q + \sum_{q=1}^{n}\tilde{\mathcal{D}}_i^{qT}P_i^q\tilde{\mathcal{D}}_i^q\Bigg)\end{aligned} \tag{68}$$

Differentiating (68) and invoking (29) yields:

$$\begin{aligned}\dot{V} = (Z^1 + \boldsymbol{\varpi})^T\dot{X}^1 + \sum_{i=1}^{N}\Bigg(\sum_{q=2}^{n}z_i^{qT}\dot{z}_i^q + \sum_{q=1}^{n-1}\boldsymbol{\varepsilon}_i^{qT}\dot{\boldsymbol{\varepsilon}}_i^q \\ + \sum_{q=1}^{n}\tilde{W}_i^{qT}\dot{\tilde{W}}_i^q + \sum_{q=1}^{n}2\tilde{\mathcal{D}}_i^{qT}P_i^q\dot{\tilde{\mathcal{D}}}_i^q\Bigg)\end{aligned} \tag{69}$$

where

$$\begin{aligned}&(Z^1 + \boldsymbol{\varpi})^T\dot{X}^1 \\ &= \sum_{l=1}^{m}(z_{1l}^1 + h_1 y_{1l}^r)\dot{x}_{1l}^1 + \sum_{l=1}^{m}(z_{2l}^1 + h_2 y_{2l}^r)\dot{x}_{2l}^1 \\ &\quad + \cdots + \sum_{l=1}^{m}(z_{Nl}^1 + h_N y_{Nl}^r)\dot{x}_{Nl}^1 \\ &= (z_1^1 + \boldsymbol{\varpi}_1)^T\dot{x}_1^1 + (z_2^1 + \boldsymbol{\varpi}_2)^T\dot{x}_2^1 \\ &\quad + \cdots + (z_N^1 + \boldsymbol{\varpi}_N)^T\dot{x}_N^1 \\ &= \sum_{i=1}^{N}(z_i^1 + \boldsymbol{\varpi}_i)^T\dot{x}_i^1\end{aligned} \tag{70}$$

Substituting (70) into (69) yields:

$$\begin{aligned}\dot{V} = \sum_{i=1}^{N}(z_i^1 + \boldsymbol{\varpi}_i)^T\dot{x}_i^1 + \sum_{i=1}^{N}\Bigg(\sum_{q=2}^{n}z_i^{qT}\dot{z}_i^q + \sum_{q=1}^{n-1}\boldsymbol{\varepsilon}_i^{qT}\dot{\boldsymbol{\varepsilon}}_i^q \\ + \sum_{q=1}^{n}\tilde{W}_i^{qT}\dot{\tilde{W}}_i^q + \sum_{q=1}^{n}2\tilde{\mathcal{D}}_i^{qT}P_i^q\dot{\tilde{\mathcal{D}}}_i^q\Bigg)\end{aligned} \tag{71}$$

According to Young's inequality and invoking (36), (38), (45), (47), (54), (56), (63), (65) and (67) yield

$$\begin{aligned}&\sum_{i=1}^{N}(z_i^1 + \boldsymbol{\varpi}_i)^T\dot{x}_i^1 \\ &= \sum_{i=1}^{N}\Big[-(z_i^1 + \boldsymbol{\varpi}_i)^T C_i^1(z_i^1 + \boldsymbol{\varpi}_i) + (z_i^1 + \boldsymbol{\varpi}_i)^T G_i^1 z_i^2 \\ &\quad + (z_i^1 + \boldsymbol{\varpi}_i)^T G_i^1\boldsymbol{\varepsilon}_i^1 + (z_i^1 + \boldsymbol{\varpi}_i)^T(\boldsymbol{\Gamma}_i^1)^{-1}(\tilde{W}_i^1\odot_m \\ &\quad \boldsymbol{\Phi}_i^1) + (z_i^1 + \boldsymbol{\varpi}_i)^T\tilde{D}_i^1\Big] \\ &\leq \sum_{i=1}^{N}\Big\{-\Big[\lambda_{\min}(C_i^1) - \frac{1}{2}(\bar{\lambda}_i^1 + 1)\Big](z_i^1 + \boldsymbol{\varpi}_i)^T(z_i^1 + \boldsymbol{\varpi}_i) \\ &\quad + (z_i^1 + \boldsymbol{\varpi}_i)^T G_i^1 z_i^2 + \frac{1}{2}\boldsymbol{\varepsilon}_i^{1T}\boldsymbol{\varepsilon}_i^1 + (z_i^1 + \boldsymbol{\varpi}_i)^T(\boldsymbol{\Gamma}_i^1)^{-1} \\ &\quad (\tilde{W}_i^1\odot_m\boldsymbol{\Phi}_i^1) + \frac{1}{2}\tilde{D}_i^{1T}\tilde{D}_i^1\Big\} \\ &\leq \sum_{i=1}^{N}\Big[-\frac{k}{2}\lambda_{\max}(\Delta)(z_i^1 + \boldsymbol{\varpi}_i)^T(z_i^1 + \boldsymbol{\varpi}_i) + (z_i^1 + \boldsymbol{\varpi}_i)^T G_i^1 \\ &\quad z_i^2 + \frac{1}{2}\boldsymbol{\varepsilon}_i^{1T}\boldsymbol{\varepsilon}_i^1 + (z_i^1 + \boldsymbol{\varpi}_i)^T(\boldsymbol{\Gamma}_i^1)^{-1}(\tilde{W}_i^1\odot_m\boldsymbol{\Phi}_i^1) \\ &\quad + \frac{1}{2}\tilde{D}_i^{1T}\tilde{D}_i^1\Big] \\ &\leq -\frac{k}{2}X^{1T}\mathcal{L}(\tilde{L})X^1 + \sum_{i=1}^{N}\Big[(z_i^1 + \boldsymbol{\varpi}_i)^T G_i^1 z_i^2 + \frac{1}{2}\boldsymbol{\varepsilon}_i^{1T}\boldsymbol{\varepsilon}_i^1 \\ &\quad (z_i^1 + \boldsymbol{\varpi}_i)^T(\boldsymbol{\Gamma}_i^1)^{-1}(\tilde{W}_i^1\odot_m\boldsymbol{\Phi}_i^1) + \frac{1}{2}\tilde{\mathcal{D}}_i^{1T}\tilde{\mathcal{D}}_i^1\Big]\end{aligned} \tag{72}$$

Similarly, using (39), (48), (57), (65) and considering Young's inequality again obtains

$$\begin{aligned}&\sum_{q=2}^{n}z_i^{q\mathrm{T}}\dot{z}_i^q \\ &= \sum_{q=2}^{n}\Big(-z_i^{q\mathrm{T}}C_i^q z_i^q + z_i^{q\mathrm{T}}\tilde{D}_i^q + z_i^{q\mathrm{T}}(\boldsymbol{\Gamma}_i^q)^{-1}(\tilde{W}_i^q\odot_m\boldsymbol{\Phi}_i^q)\Big) \\ &\quad + \sum_{q=2}^{n-1}z_i^{q\mathrm{T}}G_i^q\boldsymbol{\varepsilon}_i^q - z_i^{2\mathrm{T}}G_i^1(z_i^1 + \boldsymbol{\varpi}_i) \\ &\leqslant \sum_{q=2}^{n}\Big(-z_i^{q\mathrm{T}}C_i^q z_i^q + \frac{1}{2}z_i^{q\mathrm{T}}z_i^q + \frac{1}{2}\tilde{D}_i^{q\mathrm{T}}\tilde{D}_i^q + \\ &\quad z_i^{q\mathrm{T}}(\boldsymbol{\Gamma}_i^q)^{-1}(\tilde{W}_i^q\odot_m\boldsymbol{\Phi}_i^q)\Big) + \sum_{q=2}^{n-1}z_i^{q\mathrm{T}}G_i^q\boldsymbol{\varepsilon}_i^q\end{aligned}$$

$$
\begin{aligned}
& - \quad z_i^{2\mathrm{T}} G_i^1 (z_i^1 + \boldsymbol{\varpi}_i) \\
& \leqslant \sum_{q=2}^{n} \Big( -z_i^{q\mathrm{T}} C_i^q z_i^q + \frac{1}{2} z_i^{q\mathrm{T}} z_i^q + \frac{1}{2} \tilde{\boldsymbol{\mathcal{D}}}_i^{q\mathrm{T}} \tilde{\boldsymbol{\mathcal{D}}}_i^q \\
& + z_i^{q\mathrm{T}} (\boldsymbol{\Gamma}_i^q)^{-1} (\tilde{W}_i^q \odot_m \boldsymbol{\Phi}_i^q) \Big) + \sum_{q=2}^{n-1} z_i^{q\mathrm{T}} G_i^q \boldsymbol{\varepsilon}_i^q \\
& - z_i^{2\mathrm{T}} G_i^1 (z_i^1 + \boldsymbol{\varpi}_i)
\end{aligned} \tag{73}
$$

Similarly, it follows from (37), (46), (55), (64) and (67) that

$$
\begin{aligned}
& \sum_{q=1}^{n} \tilde{W}_i^{q\mathrm{T}} \dot{\tilde{W}}_i^q \\
& = -\sum_{q=1}^{n} \tilde{W}_i^{q\mathrm{T}} \dot{\hat{W}}_i^q \\
& = -\tilde{W}_i^{1\mathrm{T}} (\boldsymbol{\Gamma}_i^1)^{-1} [\boldsymbol{\Phi}_i^1 \odot (z_i^1 + \boldsymbol{\varpi}_i)] - \sum_{q=2}^{n} \tilde{W}_i^{q\mathrm{T}} (\boldsymbol{\Gamma}_i^q)^{-1} \\
& \quad (\boldsymbol{\Phi}_i^q \odot z_i^q) + \sum_{q=1}^{n} \lambda_i^q \tilde{W}_i^{q\mathrm{T}} \hat{W}_i^q \\
& \leqslant -\tilde{W}_i^{1\mathrm{T}} (\boldsymbol{\Gamma}_i^1)^{-1} [\boldsymbol{\Phi}_i^1 \odot (z_i^1 + \boldsymbol{\varpi}_i)] - \sum_{q=2}^{n} \tilde{W}_i^{q\mathrm{T}} (\boldsymbol{\Gamma}_i^q)^{-1} \\
& \quad (\boldsymbol{\Phi}_i^q \odot z_i^q) + \sum_{q=1}^{n} \Big[ -\lambda_i^q (1 - \frac{1}{2\pi_i^q}) \tilde{W}_i^{q\mathrm{T}} \tilde{W}_i^q + \\
& \quad + \frac{\lambda_i^q \pi_i^q}{2} \| W_i^{q*} \|^2 \Big]
\end{aligned} \tag{74}
$$

$$
\begin{aligned}
& \sum_{q=1}^{n-1} \boldsymbol{\varepsilon}_i^{q\mathrm{T}} \dot{\boldsymbol{\varepsilon}}_i^q \\
& \leqslant \sum_{q=1}^{n-1} \Big( -\boldsymbol{\varepsilon}_i^{q\mathrm{T}} (\boldsymbol{\Upsilon}_i^q)^{-1} \boldsymbol{\varepsilon}_i^q + \boldsymbol{\varepsilon}_i^{q\mathrm{T}} \bar{B}_i^q \Big) \\
& \leqslant \sum_{q=1}^{n-1} \Big( -\boldsymbol{\varepsilon}_i^{q\mathrm{T}} (\boldsymbol{\Upsilon}_i^q)^{-1} \boldsymbol{\varepsilon}_i^q + \frac{1}{2} \boldsymbol{\varepsilon}_i^{q\mathrm{T}} \boldsymbol{\varepsilon}_i^q + \frac{1}{2} \bar{B}_i^{q\mathrm{T}} \bar{B}_i^q \Big)
\end{aligned} \tag{75}
$$

Similarly, by applying Lemma 3, (34), (44), (53) and (62), it can be derived that

$$
\begin{aligned}
& \sum_{q=1}^{n} 2 \tilde{\boldsymbol{\mathcal{D}}}_i^{qT} P_i^q \dot{\tilde{\boldsymbol{\mathcal{D}}}}_i^q \\
& = \sum_{q=1}^{n} 2 \tilde{\boldsymbol{\mathcal{D}}}_i^{qT} P_i^q \Big( K_i^q \tilde{\boldsymbol{\mathcal{D}}}_i^q + \boldsymbol{\mathcal{D}}_i^{q*} \\
& \quad + K_i^{q*} \otimes \Big( (\boldsymbol{\Gamma}_i^q)^{-1} (\tilde{W}_i^q \odot \boldsymbol{\Phi}_i^q) \Big) \Big) \\
& = \sum_{q=1}^{n} \Big[ \tilde{\boldsymbol{\mathcal{D}}}_i^{qT} (K_i^{qT} P_i^q + P_i^{qT} K_i^q) \tilde{\boldsymbol{\mathcal{D}}}_i^q + \tilde{\boldsymbol{\mathcal{D}}}_i^{qT} P_i^q \boldsymbol{\mathcal{D}}_i^{q*} \\
& + \quad \boldsymbol{\mathcal{D}}_i^{q*T} P_i^q \tilde{\boldsymbol{\mathcal{D}}}_i^q + \tilde{\boldsymbol{\mathcal{D}}}_i^{qT} P_i^q \Big( K_i^{q*} \otimes \Big( (\boldsymbol{\Gamma}_i^q)^{-1} (\tilde{W}_i^q \odot_m \\
& \quad \boldsymbol{\Phi}_i^q)) \Big) + \Big( K_i^{q*} \otimes \Big( (\boldsymbol{\Gamma}_i^q)^{-1} (\tilde{W}_i^q \odot_m \boldsymbol{\Phi}_i^q) \Big) \Big)^T P_i^{qT} \tilde{\boldsymbol{\mathcal{D}}}_i^q \Big] \\
& \leq \sum_{q=1}^{n} \Big[ \tilde{\boldsymbol{\mathcal{D}}}_i^{qT} (K_i^{qT} P_i^q + P_i^{qT} K_i^q) \tilde{\boldsymbol{\mathcal{D}}}_i^q + a_i^q \boldsymbol{\mathcal{D}}_i^{q*T} \boldsymbol{\mathcal{D}}_i^{q*} \\
& \quad + (a_i^q)^{-1} \tilde{\boldsymbol{\mathcal{D}}}_i^{qT} P_i^q P_i^{qT} \tilde{\boldsymbol{\mathcal{D}}}_i^q + b_i^q \textstyle\sum_{\ell=1}^{r} \Big( (\tilde{W}_i^q \odot_m \boldsymbol{\Phi}_i^q)^T \\
& \quad (\boldsymbol{\Gamma}_i^q)^{-1} k_i^{q\ell T} \Big) \Big( k_i^{q\ell} (\boldsymbol{\Gamma}_i^q)^{-1} (\tilde{W}_i^q \odot_m \boldsymbol{\Phi}_i^q) \Big) \\
& \quad + \quad (b_i^q)^{-1} \tilde{\boldsymbol{\mathcal{D}}}_i^{qT} P_i^q P_i^{qT} \tilde{\boldsymbol{\mathcal{D}}}_i^q \Big] \\
& \leq \sum_{q=1}^{n} \Big[ \tilde{\boldsymbol{\mathcal{D}}}_i^{qT} (K_i^{qT} P_i^q + P_i^{qT} K_i^q) \tilde{\boldsymbol{\mathcal{D}}}_i^q + (a_i^q)^{-1} \tilde{\boldsymbol{\mathcal{D}}}_i^{qT} P_i^q \\
& \quad P_i^{qT} \tilde{\boldsymbol{\mathcal{D}}}_i^q + a_i^q (\beta_i^{qr})^2 + b_i^q \textstyle\sum_{\ell=1}^{r} \iota_i^q \lambda_{\max} \Big( (\boldsymbol{\Gamma}_i^q)^{-1} k_i^{q\ell T} \\
& \quad k_i^{q\ell} (\boldsymbol{\Gamma}_i^q)^{-1} \Big) \tilde{W}_i^{qT} \tilde{W}_i^q + (b_i^q)^{-1} \tilde{\boldsymbol{\mathcal{D}}}_i^{qT} P_i^q P_i^{qT} \tilde{\boldsymbol{\mathcal{D}}}_i^q \Big]
\end{aligned} \tag{76}
$$

Then, it follows from (72), (73), (74), (75) and (76) that the time derivative of $V$ can be expressed as follows:

$$
\begin{aligned}
\dot{V} & \leq \sum_{i=1}^{N} (z_i^1 + \boldsymbol{\varpi}_i)^T \dot{x}_i^1 + \sum_{i=1}^{N} \Big( \sum_{q=2}^{n} z_i^{qT} \dot{z}_i^q \\
& + \quad \sum_{q=1}^{n-1} \boldsymbol{\varepsilon}_i^{qT} \dot{\boldsymbol{\varepsilon}}_i^q + \sum_{q=1}^{n} \tilde{W}_i^{qT} \dot{\tilde{W}}_i^q + \sum_{q=1}^{n} 2 \tilde{\boldsymbol{\mathcal{D}}}_i^{qT} P_i^q \dot{\tilde{\boldsymbol{\mathcal{D}}}}_i^q \Big) \\
& \leq -\frac{k}{2} X^{1T} \mathcal{L}(\tilde{L}) X^1 + \sum_{i=1}^{N} \Big\{ \frac{1}{2} \boldsymbol{\varepsilon}_i^{1T} \boldsymbol{\varepsilon}_i^1 + \sum_{q=2}^{n} \Big( -z_i^{qT} C_i^q z_i^q \\
& + \quad \frac{1}{2} z_i^{qT} z_i^q \Big) + \sum_{q=1}^{n} \frac{1}{2} \tilde{\boldsymbol{\mathcal{D}}}_i^{qT} \tilde{\boldsymbol{\mathcal{D}}}_i^q + \sum_{q=2}^{n-1} z_i^{qT} G_i^q \boldsymbol{\varepsilon}_i^q \\
& + \quad \sum_{q=1}^{n-1} \Big( -\boldsymbol{\varepsilon}_i^{qT} (\boldsymbol{\Upsilon}_i^q)^{-1} \boldsymbol{\varepsilon}_i^q + \frac{1}{2} \boldsymbol{\varepsilon}_i^{qT} \boldsymbol{\varepsilon}_i^q + \frac{1}{2} \bar{B}_i^{qT} \bar{B}_i^q \Big) \\
& + \quad \sum_{q=1}^{n} \Big[ -\lambda_i^q (1 - \frac{1}{2\pi_i^q}) \tilde{W}_i^{qT} \tilde{W}_i^q + \frac{\lambda_i^q \pi_i^q}{2} \| W_i^{q*} \|^2 \Big] \\
& + \quad \sum_{q=1}^{n} \Big[ \tilde{\boldsymbol{\mathcal{D}}}_i^{qT} (K_i^{qT} P_i^q + P_i^{qT} K_i^q) \tilde{\boldsymbol{\mathcal{D}}}_i^q + (a_i^q)^{-1} \tilde{\boldsymbol{\mathcal{D}}}_i^{qT} P_i^q \\
& \quad P_i^{qT} \tilde{\boldsymbol{\mathcal{D}}}_i^q + a_i^q (\beta_i^{qr})^2 + b_i^q \textstyle\sum_{\ell=1}^{r} \iota_i^q \lambda_{\max} \Big( (\boldsymbol{\Gamma}_i^q)^{-1} k_i^{q\ell T} \\
& \quad k_i^{q\ell} (\boldsymbol{\Gamma}_i^q)^{-1} \Big) \tilde{W}_i^{qT} \tilde{W}_i^q + (b_i^q)^{-1} \tilde{\boldsymbol{\mathcal{D}}}_i^{qT} P_i^q P_i^{qT} \tilde{\boldsymbol{\mathcal{D}}}_i^q \Big] \Big\} \\
& \leq -\frac{k}{2} X^{1T} \mathcal{L}(\tilde{L}) X^1 - \sum_{i=1}^{N} \Big[ \sum_{q=2}^{n-1} \Big( \lambda_{\min}(C_i^q) - \frac{1}{2} (\bar{\lambda}_i^q + 1) \Big) \\
& \quad z_i^{qT} z_i^q + \Big( \lambda_{\min}(C_i^n) - \frac{1}{2} \Big) z_i^{nT} z_i^n \Big] \\
& \quad - \sum_{i=1}^{N} \Big[ \sum_{q=1}^{n-1} \Big( \lambda_{\min}(\boldsymbol{\Upsilon}_i^q)^{-1} \\
& \quad -1 \Big) \boldsymbol{\varepsilon}_i^{qT} \boldsymbol{\varepsilon}_i^q \Big] - \sum_{i=1}^{N} \Big[ \sum_{q=1}^{n} \tilde{\boldsymbol{\mathcal{D}}}_i^{qT} \Big( -(K_i^{qT} P_i^q + P_i^{qT} K_i^q)
\end{aligned}
$$

$$
\begin{aligned}
&- \frac{1}{2}I_{mr\times mr} - \left((a_i^q)^{-1} + (b_i^q)^{-1}\right) P_i^{qT} P_i^q\Big) \tilde{\mathcal{D}}_i^q\Big] \\
&- \sum_{i=1}^{N}\left[\sum_{q=1}^{n} \tilde{W}_i^{qT}\left(\lambda_i^q(1 - \frac{1}{2\pi_i^q}) - b_i^q \sum\nolimits_{\ell=1}^{r} \iota_i^q \lambda_{\max}\right.\right. \\
&\quad \left.\left.\left((\boldsymbol{\Gamma}_i^q)^{-1} k_i^{q\ell T} k_i^{q\ell} (\boldsymbol{\Gamma}_i^q)^{-1}\right)\right) \tilde{W}_i^q\right] + \sum_{i=1}^{N}\left[\sum_{q=1}^{n-1}\frac{1}{2}\bar{B}_i^{qT}\right. \\
&\quad \left.\bar{B}_i^q + \sum_{q=1}^{n}\left(a_i^q(\beta_i^{qr})^2 + \frac{\lambda_i^q\pi_i^q}{2}\|W_i^{q*}\|^2\right)\right] \\
&\le -\kappa V + M
\end{aligned}
\tag{77}
$$

where

$$
\begin{aligned}
\kappa = \min &\Big\{k, \lambda_{\min}(C_i^q) - \frac{1}{2}(\bar{\lambda}_i^q + 1), \lambda_{\min}(C_i^n) - \frac{1}{2}, \\
&\lambda_{\min}(\boldsymbol{\Upsilon}_i^q)^{-1} - 1, \lambda_{\min}\Big(-(K_i^{qT} P_i^q + P_i^{qT} K_i^q) - \\
&\frac{1}{2}I_{mr\times mr} - \left((a_i^q)^{-1} + (b_i^q)^{-1}\right) P_i^{qT} P_i^q\Big), \lambda_i^q(1 \\
&- \frac{1}{2\pi_i^q}) - b_i^q \sum\nolimits_{\ell=1}^{r} \iota_i^q \lambda_{\max}\left((\boldsymbol{\Gamma}_i^q)^{-1} k_i^{q\ell T} k_i^{q\ell} (\boldsymbol{\Gamma}_i^q)^{-1}\right)\Big\} \\
&>0
\end{aligned}
$$

$$
\begin{aligned}
M = &\sum_{i=1}^{N}\left[\sum_{q=1}^{n-1}\frac{1}{2}\bar{B}_i^{qT}\bar{B}_i^q + \sum_{q=1}^{n}\left(a_i^q(\beta_i^{qr})^2\right.\right. \\
&\left.\left. + \frac{\lambda_i^q\pi_i^q}{2}\left\|W_i^{q*}\right\|^2\right)\right], \quad q = 1, 2, \cdots n
\end{aligned}
$$

Therefore, it follows from Lemma 1 that the signals of the closed-loop system are SGUUB. It is easy to deduce from (77) that

$$
0 \le V(t) \le e^{-\kappa t}V(0) + \frac{M}{\kappa}(1 - e^{-\kappa t}) \tag{78}
$$

It follows from (78) that there exists a moment $T_0$ such that for any $t > T_0$, signals $X^1$, $z_i^q$, $\tilde{W}_i^q$, and $\tilde{\mathcal{D}}_i^q$ are invariant to the compact sets defined as follows:

$$
\Omega_{X^1} = \left(X^1 \,\middle|\, \left\|X^1\right\| \le \sqrt{2M/\lambda_{\max}(\Lambda)\cdot\kappa}\right) \tag{79}
$$

$$
\Omega_{z_i^q} = \left(z_i^q \mid \|z_i^q\| \le \sqrt{2M/\kappa}\right) \tag{80}
$$

$$
\Omega_{\tilde{W}_i^q} = \left(\tilde{W}_i^q \,\middle|\, \left\|\tilde{W}_i^q\right\| \le \sqrt{2M/\kappa}\right) \tag{81}
$$

$$
\Omega_{\tilde{\mathcal{D}}_i^q} = \left(\tilde{\mathcal{D}}_i^q \,\middle|\, \left\|\tilde{\mathcal{D}}_i^q\right\| \le \sqrt{M/\lambda_{\max}(P_i^q)\cdot\kappa}\right) \tag{82}
$$

By increasing the values of $\kappa$, the quantities $\sqrt{2M/\lambda_{\max}(\Lambda)\cdot\kappa}$, $\sqrt{2M/\kappa}$ and $\sqrt{M/\lambda_{\max}(P_i^q)\cdot\kappa}$ can be made arbitrarily small. This concludes the proof.

## IV. SIMULATION RESULTS

In this section, simulations are performed to verify the effectiveness of the proposed distributed anti-disturbance cooperative control protocol. A quadrotor UAV formation with one virtual leader and four followers is considered. The topology is shown in Figure 2. Node 0 is the virtual leader that sends the signal, and nodes 1-4 are the followers. It assumes that that the weights of all edges are 1, the degree matrix $\mathcal{B} = diag\{2, 1, 2, 1\}$ is obtained, and the adjacency weight matrix A and Laplace matrix of the followers are as follows:

$$
\mathcal{A} = \begin{bmatrix} 0 & 1 & 1 & 0 \\ 1 & 0 & 0 & 0 \\ 1 & 0 & 0 & 1 \\ 0 & 0 & 1 & 0 \end{bmatrix}, \quad L = \begin{bmatrix} 2 & -1 & -1 & 0 \\ -1 & 1 & 0 & 0 \\ -1 & 0 & 2 & -1 \\ 0 & 0 & -1 & 1 \end{bmatrix}
$$

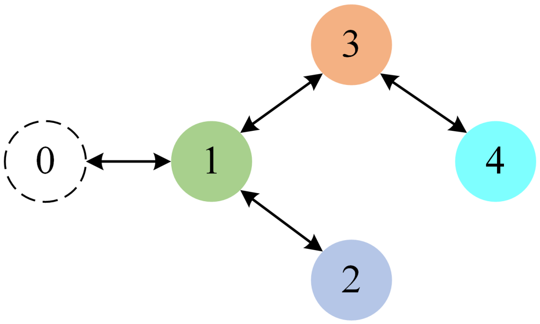

**FIGURE 2.** Communication topology diagram.

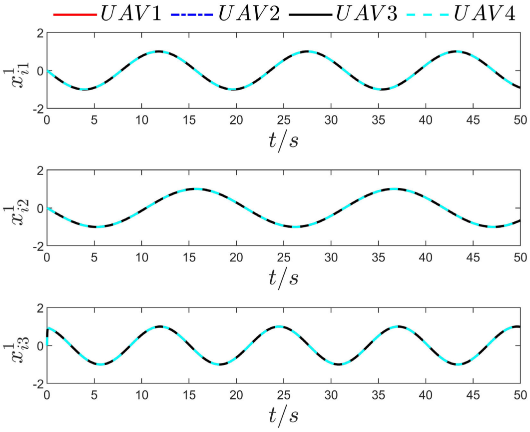

**FIGURE 3.** Tracking effect of followers.

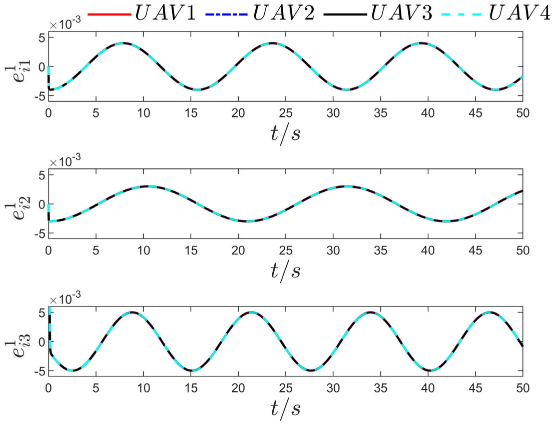

**FIGURE 4.** Tracking error of followers to leaders.

**TABLE 1.** Other parameters and controller design parameters.

| Agent | $UAV1$ | $UAV2$ | $UAV3$ | $UAV4$ |
|---|---|---|---|---|
| $\Delta f_i^2$ | $[0.1\dot\phi_1,\ 0.1\dot\theta_1,\ 0.1\dot\psi_1]^{\mathrm{T}}$ | $[0.2\dot\phi_2,\ 0.2\dot\theta_2,\ 0.2\dot\psi_2]^{\mathrm{T}}$ | $[0.3\dot\phi_3,\ 0.3\dot\theta_3,\ 0.3\dot\psi_3]^{\mathrm{T}}$ | $[0.4\dot\phi_4,\ 0.4\dot\theta_4,\ 0.4\dot\psi_4]^{\mathrm{T}}$ |
| $d_i^2$ | $\begin{bmatrix} 2\sin t + 15 \\ 2\cos t + 15 \\ 2\cos(2t) + 15 \end{bmatrix}$ | $\begin{bmatrix} 5\sin(0.5t) + 10 \\ 2\cos(0.9t) + 8 \\ 2\cos(0.6t) + 10 \end{bmatrix}$ | $\begin{bmatrix} 8\sin(0.5t) + 5 \\ 3\cos(0.9t) + 10 \\ 2\cos(0.7t) + 10 \end{bmatrix}$ | $\begin{bmatrix} 8\sin(0.5t) + 10 \\ 5\cos(0.8t) + 10 \\ 6\cos(0.6t) + 10 \end{bmatrix}$ |
| $C_i^1$ | $diag(100, 100, 100)$ | $diag(100, 100, 100)$ | $diag(100, 100, 100)$ | $diag(100, 100, 100)$ |
| $k_i^{21}$ | $diag(100, 100, 100)$ | $diag(100, 100, 100)$ | $diag(100, 100, 100)$ | $diag(100, 100, 100)$ |
| $k_i^{22}$ | $diag(100, 100, 100)$ | $diag(100, 100, 100)$ | $diag(100, 100, 100)$ | $diag(100, 100, 100)$ |
| $C_i^2$ | $diag(200, 200, 200)$ | $diag(200, 200, 200)$ | $diag(200, 200, 200)$ | $diag(200, 200, 200)$ |

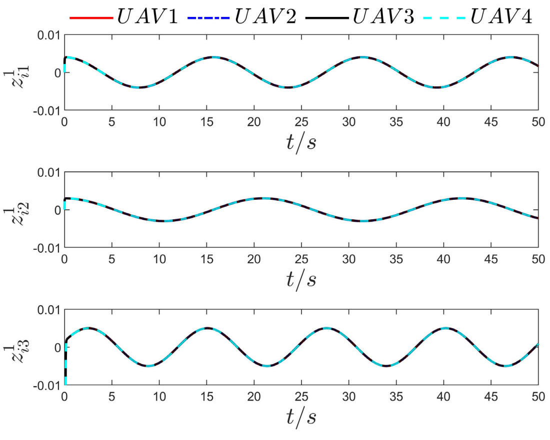

**FIGURE 5.** Consensus error of followers.

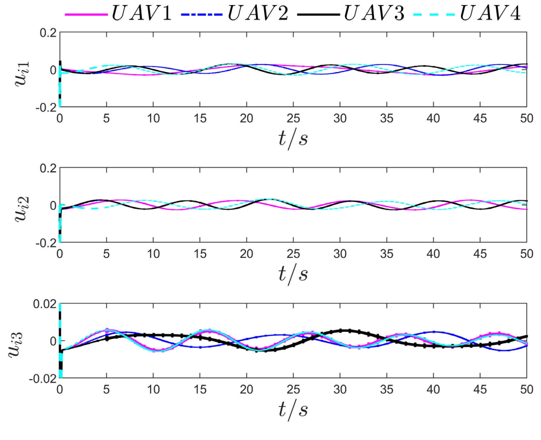

**FIGURE 6.** Control input of followers.

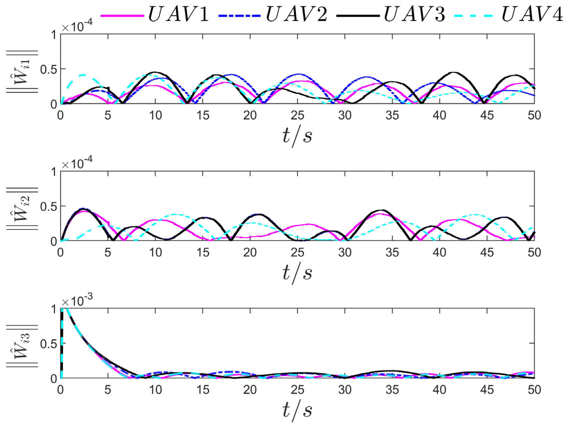

**FIGURE 7.** Norm of NN weights.

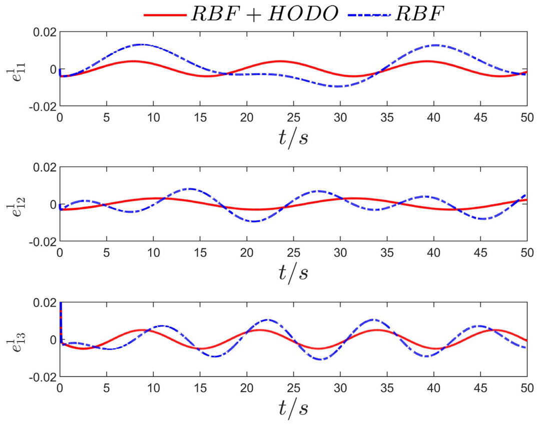

**FIGURE 8.** Comparative tracking errors of UAV1.

Let $H = diag\{1, 0, 0, 0\}$, $\mathcal{L}(\tilde{L}) = \mathcal{L}(L + H) = \mathcal{L}(L) + \mathcal{L}(H)$, and $\lambda_{\max}(\Delta) = 4.4142$. The attitude dynamics of the $i^{th}$ UAV are modeled as follows:

$$\begin{cases} \dot{x}_i^1 = x_i^2 \\ \dot{x}_i^2 = F_i^2(\bar{x}_i^2) + G_i^2 u_i + \Delta f_i^2(\bar{x}_i^2) + d_i^2(\bar{x}_i^2, t) \\ y_i = x_i^1 \end{cases}$$

where $x_i^1 = [\phi_i, \theta_i, \psi_i]^T$, and $\phi_i$, $\theta_i$ and $\theta_i$ denote the roll angle, pitch angle and yaw angle of the $i^{th}$ quadrotor UAV, respectively. $F_i^2(\bar{x}_i^2) = [(\dot\theta\dot\psi(I_{i\theta} - I_{i\psi}))/I_{i\phi}, (\dot\phi\dot\psi(I_{i\psi} - I_{i\phi}))/I_{i\theta}, (\dot\theta\dot\phi(I_{i\phi} - I_{i\theta}))/I_{i\psi}]^T$, $I_{i\phi} = 0.00623$, $I_{i\theta} = 0.00623$, and $I_{i\psi} = 0.00112$ denote the moments of inertia of the $i^{th}$ quadrotor UAV. $G_i^2 = diag(l/I_{i\phi}, l/I_{i\theta}, l/I_{i\psi})$ and $l = 0.26m$ is the distance from the rotor to the center of mass of the UAV. $\Delta f_i^2$ and $d_i^2$ are the internal uncertainty and external disturbance of the $i^{th}$ UAV, respectively. The desired reference signal is $y^d = [\sin(0.4t + \pi), \cos(0.3t + 0.5\pi), \sin(0.5t + 0.6\pi)]^T$, and

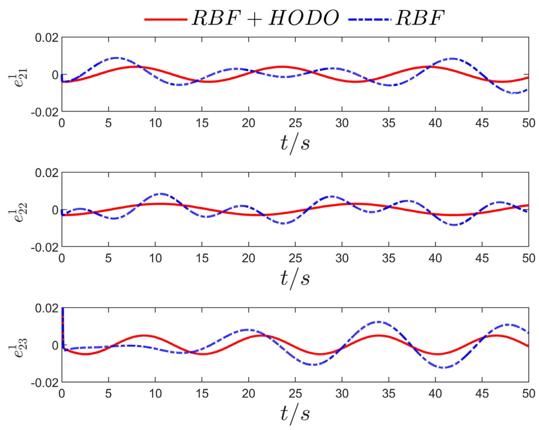

**FIGURE 9.** Comparative tracking errors of UAV2.

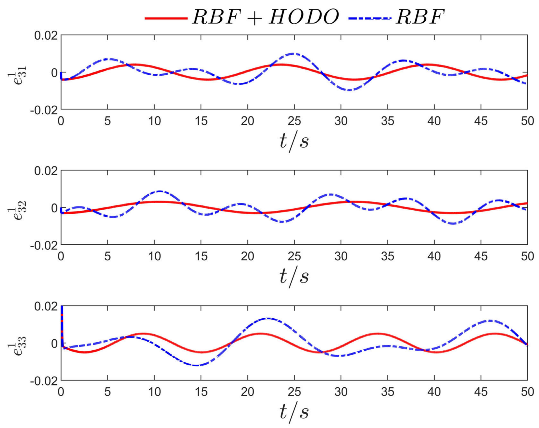

**FIGURE 10.** Comparative tracking errors of UAV3.

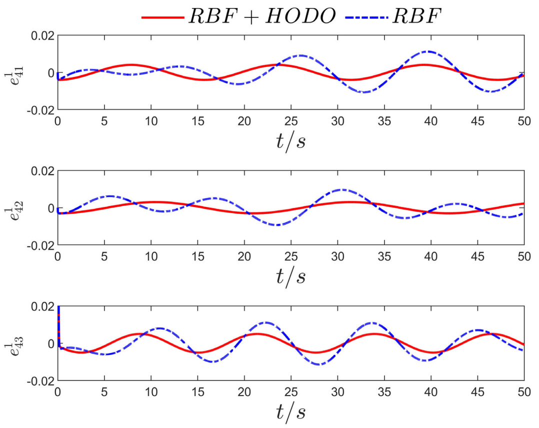

**FIGURE 11.** Comparative tracking errors of UAV4.

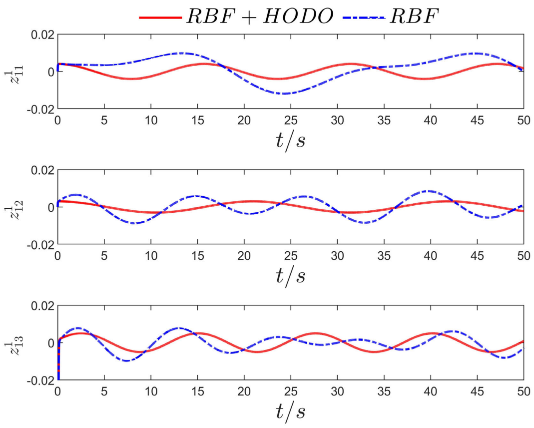

**FIGURE 12.** Comparative consensus errors of UAV1.

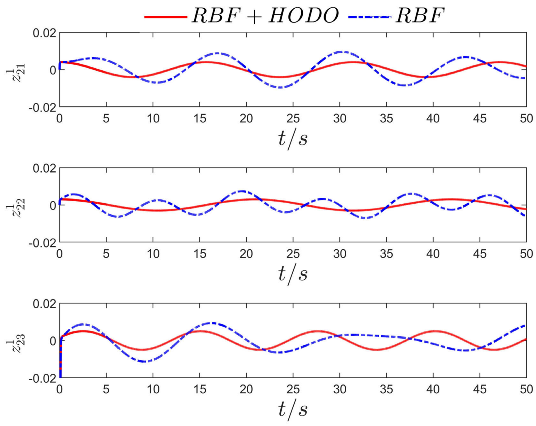

**FIGURE 13.** Comparative consensus errors of UAV2.

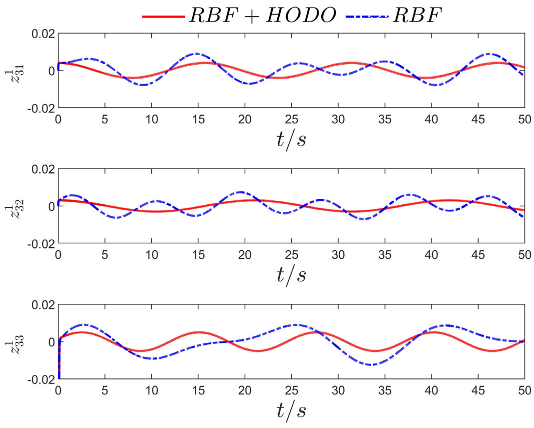

**FIGURE 14.** Comparative consensus errors of UAV3.

the initial values for each UAV are $x_{1,0} = [0, 0, 0, 0, 0, 0]^T$, $x_{2,0} = [5, 5, 5, 0, 0, 0]^T$, $x_{3,0} = [10, 10, 10, 0, 0, 0]^T$ and $x_{4,0} = [15, 15, 15, 0, 0, 0]^T$. The Gaussian width of the RBFNN is chosen to be $\bar{b} = 1$, the neuron Gaussian center is taken as $\bar{c}_i \in [-3, 3]$, $\hat{W}_i^2(0) = 0$, $\bar{\ell}_i^2 = 7$ is the number of neuron rules and the updating law-related parameters are taken to be $\mathbf{\Gamma}_i^2 = diag(10, 10, 10)$ and $\lambda_i^2 = 2$. The parameter $k_i$ is chosen to be $k_i = 2$, and the other parameters and controller design parameters are shown in Table 1. From the parameters in Table 1, the parameter $C_i^1$ satisfies $\lambda_{\min}(C_i^1) \geq \frac{k_i}{2}\lambda_{\max}(\Delta) + \frac{1}{2}(\bar{\lambda}_i^1 + 1)$.

The simulation results show the performance of the proposed distributed anti-disturbance cooperative control protocol in Figs. 3-15. Figs. 3 and 4 show the tracking results and tracking error, respectively. Fig. 5 shows the consensus error of the quadrotor UAV formation, and Fig. 6 shows the control input of the system. The tracking error converges within ±0.5%, and the consensus error converges

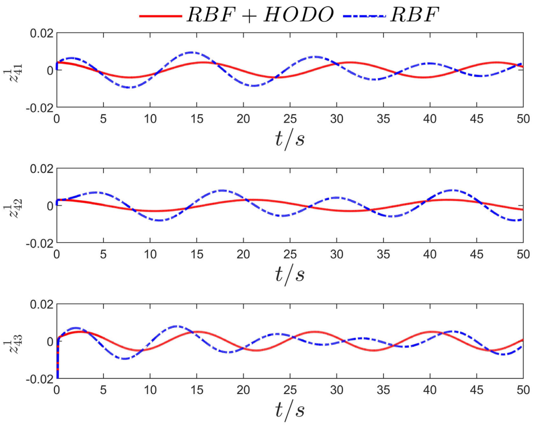

**FIGURE 15.** **Comparative consensus errors of UAV4.**

within ±1%, which shows that the distributed controller designed in this paper has a good tracking effect on quadrotor UAV formation. Figs. 8-11 and Figs. 12-15 compare the tracking error and consensus error for the four UAVs with an HODO (red solid line) and without an HODO (blue dashed line) controller, respectively. Although the RBFNN-only distributed controller also has a good tracking effect - the error converges to within ±2% - the HODO-supported distributed controller converges to a smaller interval, and the vibration is smoother, which gives a better tracking effect. In addition, although the NN also has a good approximation capability, it is only effective on the compact set. Considering that the range of unknown disturbances is difficult to recognize in reality, there is a possibility that the neural network fails. With the help of HODO, this risk could be avoided. By the simulation results, the proposed distributed anti-disturbance cooperative control protocol can fulfill the consensus assignment for high-order MIMO nonlinear MASs.

## V. CONCLUSION

In this paper, a distributed adaptive anti-disturbance cooperative control scheme is proposed for a class of high-order MIMO nonlinear MASs subjected to uncertainties and external disturbances. An RBFNN is used to approximate the system uncertainties, and an HODO is used to estimate the compounded disturbances. By analyzing the relationships among the Laplace matrix, leader-following adjacency matrix and consensus tracking error, an appropriate Lyapunov function is constructed to guarantee that the control protocol has the properties of simple structure, low computational burden and signal boundedness of closed-loop systems. If the communication topology is a directed graph, the designed control method will be more meaningful. In the future, the distributed anti-disturbance cooperative control protocol for high-order MIMO nonlinear MASs will be considered in the presence of directed graphs, dynamic topologies and practical engineering applications. In addition, the parameter optimization methods will be investigated in the controller design process.

## REFERENCES

[1] K.-K. Oh, M.-C. Park, and H.-S. Ahn, "A survey of multi-agent formation control," *Automatica*, vol. 53, pp. 424–440, Mar. 2015.

[2] J. Thunberg, J. Goncalves, and X. Hu, "Consensus and formation control on *SE* (3) for switching topologies," *Automatica*, vol. 66, pp. 109–121, Apr. 2016.

[3] P. Dasgupta, "A multiagent swarming system for distributed automatic target recognition using unmanned aerial vehicles," *IEEE Trans. Syst., Man, Cybern. A, Syst., Humans*, vol. 38, no. 3, pp. 549–563, May 2008.

[4] H. Shi, L. Wang, and T. Chu, "Swarming behavior of multi-agent systems," *J. Control Theory Appl.*, vol. 2, no. 4, pp. 313–318, Nov. 2004.

[5] J. Qin, W. Fu, H. Gao, and W. X. Zheng, "Distributed $k$-means algorithm and fuzzy $c$-means algorithm for sensor networks based on multiagent consensus theory," *IEEE Trans. Cybern.*, vol. 47, no. 3, pp. 772–783, Mar. 2017.

[6] X. Li, X. Hu, R. Zhang, and L. Yang, "Routing protocol design for underwater optical wireless sensor networks: A multiagent reinforcement learning approach," *IEEE Internet Things J.*, vol. 7, no. 10, pp. 9805–9818, Oct. 2020.

[7] S. A. Putra, B. R. Trilaksono, M. Riyansyah, D. S. Laila, A. Harsoyo, and A. I. Kistijantoro, "Intelligent sensing in multiagent-based wireless sensor network for bridge condition monitoring system," *IEEE Internet Things J.*, vol. 6, no. 3, pp. 5397–5410, Jun. 2019.

[8] C. S. K. Yeung, A. S. Y. Poon, and F. F. Wu, "Game theoretical multi-agent modelling of coalition formation for multilateral trades," *IEEE Trans. Power Syst.*, vol. 14, no. 3, pp. 929–934, Aug. 1999.

[9] Z. Lin, L. Wang, Z. Han, and M. Fu, "Distributed formation control of multi-agent systems using complex Laplacian," *IEEE Trans. Autom. Control*, vol. 59, no. 7, pp. 1765–1777, Jul. 2014.

[10] X.-F. Qiu, Y.-X. Zhang, and K.-Z. Li, "Successive lag cluster consensus on multi-agent systems via delay-dependent impulsive control," *Chin. Phys. B*, vol. 28, no. 5, May 2019, Art. no. 050501.

[11] Y. Hong, J. Hu, and L. Gao, "Tracking control for multi-agent consensus with an active leader and variable topology," *Automatica*, vol. 42, no. 7, pp. 1177–1182, Jul. 2006.

[12] P. Lin and Y. Jia, "Multi-agent consensus with diverse time-delays and jointly-connected topologies," *Automatica*, vol. 47, no. 4, pp. 848–856, Apr. 2011.

[13] W. Ren and R. W. Beard, "Consensus seeking in multiagent systems under dynamically changing interaction topologies," *IEEE Trans. Autom. Control*, vol. 50, no. 5, pp. 655–661, May 2005.

[14] V. D. Blondel, J. M. Hendrickx, and J. N. Tsitsiklis, "On Krause's multi-agent consensus model with state-dependent connectivity," *IEEE Trans. Autom. Control*, vol. 54, no. 11, pp. 2586–2597, Nov. 2009.

[15] F. Wang, H. Yang, Z. Liu, and Z. Chen, "Containment control of leader-following multi-agent systems with jointly-connected topologies and time-varying delays," *Neurocomputing*, vol. 260, pp. 341–348, Oct. 2017.

[16] Y. Hong, G. Chen, and L. Bushnell, "Distributed observers design for leader-following control of multi-agent networks," *Automatica*, vol. 44, no. 3, pp. 846–850, Mar. 2008.

[17] Z. Li, X. Liu, P. Lin, and W. Ren, "Consensus of linear multi-agent systems with reduced-order observer-based protocols," *Syst. Control Lett.*, vol. 60, no. 7, pp. 510–516, Jul. 2011.

[18] W. Yu, L. Zhou, X. Yu, J. Lu, and R. Lu, "Consensus in multi-agent systems with second-order dynamics and sampled data," *IEEE Trans. Ind. Informat.*, vol. 9, no. 4, pp. 2137–2146, Nov. 2013.

[19] H. Zhang, G. Feng, H. Yan, and Q. Chen, "Observer-based output feedback event-triggered control for consensus of multi-agent systems," *IEEE Trans. Ind. Electron.*, vol. 61, no. 9, pp. 4885–4894, Sep. 2014.

[20] X. Wang and G.-H. Yang, "Fault-tolerant consensus tracking control for linear multiagent systems under switching directed network," *IEEE Trans. Cybern.*, vol. 50, no. 5, pp. 1921–1930, May 2020.

[21] G. Cui, H. Xu, X. Chen, and J. Yu, "Fixed-time distributed adaptive formation control for multiple QUAVs with full-state constraints," *IEEE Trans. Aerosp. Electron. Syst.*, vol. 59, no. 4, pp. 4192–4206, Aug. 2023.

[22] S. Ghapani, S. Rahili, and W. Ren, "Distributed average tracking of physical second-order agents with heterogeneous unknown nonlinear dynamics without constraint on input signals," *IEEE Trans. Autom. Control*, vol. 64, no. 3, pp. 1178–1184, Mar. 2019.

[23] M. Chen and S. S. Ge, "Direct adaptive neural control for a class of uncertain nonaffine nonlinear systems based on disturbance observer," *IEEE Trans. Cybern.*, vol. 43, no. 4, pp. 1213–1225, Aug. 2013.

[24] G. Cui, H. Xu, J. Yu, and H.-K. Lam, "Event-triggered distributed fixed-time adaptive attitude control with prescribed performance for multiple QUAVs," *IEEE Trans. Autom. Sci. Eng.*, early access, Aug. 1, 2023, doi: 10.1109/TASE.2023.3297235.

[25] Q. Shen, P. Shi, J. Zhu, S. Wang, and Y. Shi, "Neural networks-based distributed adaptive control of nonlinear multiagent systems," *IEEE Trans. Neural Netw. Learn. Syst.*, vol. 31, no. 3, pp. 1010–1021, Mar. 2020.

[26] W. Meng, Q. Yang, J. Si, and Y. Sun, "Consensus control of nonlinear multiagent systems with time-varying state constraints," *IEEE Trans. Cybern.*, vol. 47, no. 8, pp. 2110–2120, Aug. 2017.

[27] K. Li and Y. Li, "Adaptive NN optimal consensus fault-tolerant control for stochastic nonlinear multiagent systems," *IEEE Trans. Neural Netw. Learn. Syst.*, vol. 34, no. 2, pp. 947–957, Feb. 2023.

[28] X. Jin, S. Lu, and J. Yu, "Adaptive NN-based consensus for a class of nonlinear multiagent systems with actuator faults and faulty networks," *IEEE Trans. Neural Netw. Learn. Syst.*, vol. 33, no. 8, pp. 3474–3486, Aug. 2022.

[29] D. Cui, C. K. Ahn, and Z. Xiang, "Fault-tolerant fuzzy observer-based fixed-time tracking control for nonlinear switched systems," *IEEE Trans. Fuzzy Syst.*, early access, Jun. 12, 2023, doi: 10.1109/TFUZZ.2023.3284917.

[30] L. Ma, F. Zhu, J. Zhang, and X. Zhao, "Leader–follower asymptotic consensus control of multiagent systems: An observer-based disturbance reconstruction approach," *IEEE Trans. Cybern.*, vol. 53, no. 2, pp. 1311–1323, Feb. 2023.

[31] D. Cui, W. Zou, J. Guo, and Z. Xiang, "Neural network-based adaptive finite-time tracking control of switched nonlinear systems with time-varying delay," *Appl. Math. Comput.*, vol. 428, Sep. 2022, Art. no. 127216.

[32] J. Yang, S. Li, and X. Yu, "Sliding-mode control for systems with mismatched uncertainties via a disturbance observer," *IEEE Trans. Ind. Electron.*, vol. 60, no. 1, pp. 160–169, Jan. 2013.

[33] W.-H. Chen, "Disturbance observer based control for nonlinear systems," *IEEE/ASME Trans. Mechatronics*, vol. 9, no. 4, pp. 706–710, Dec. 2004.

[34] K. Ohnishi, "A new servo method in mechatronics," *Trans. Jpn. Soc. Electr. Eng. D*, vol. 177, pp. 83–86, 1987.

[35] A. Mohammadi, H. J. Marquez, and M. Tavakoli, "Nonlinear disturbance observers: Design and applications to Euler? Lagrange systems," *IEEE Control Syst. Mag.*, vol. 37, no. 4, pp. 50–72, Jul. 2017.

[36] W. Bai, G. Chen, Q. Zhou, and R. Lu, "Disturbance-observer-based event-triggered control for multi-agent systems with input saturation," *Scientia Sinica Informationis*, vol. 49, no. 11, pp. 1502–1516, Nov. 2019.

[37] N. Ahmed, M. Chen, and S. Shao, "Disturbance observer based tracking control of quadrotor with high-order disturbances," *IEEE Access*, vol. 8, pp. 8300–8313, 2020.

[38] K.-S. Kim, K.-H. Rew, and S. Kim, "Disturbance observer for estimating higher order disturbances in time series expansion," *IEEE Trans. Autom. Control*, vol. 55, no. 8, pp. 1905–1911, Aug. 2010.

[39] W. Zheng and M. Chen, "Tracking control of manipulator based on high-order disturbance observer," *IEEE Access*, vol. 6, pp. 26753–26764, 2018.

[40] J. Huang, M. Zhang, S. Ri, C. Xiong, Z. Li, and Y. Kang, "High-order disturbance-observer-based sliding mode control for mobile wheeled inverted pendulum systems," *IEEE Trans. Ind. Electron.*, vol. 67, no. 3, pp. 2030–2041, Mar. 2020.

[41] H. Zhang and F. L. Lewis, "Adaptive cooperative tracking control of higher-order nonlinear systems with unknown dynamics," *Automatica*, vol. 48, no. 7, pp. 1432–1439, Jul. 2012.

[42] S. Tong and Y. Li, "Adaptive fuzzy output feedback control of MIMO nonlinear systems with unknown dead-zone inputs," *IEEE Trans. Fuzzy Syst.*, vol. 21, no. 1, pp. 134–146, Feb. 2013.

[43] T. Madani and A. Benallegue, "Adaptive control via backstepping technique and neural networks of a quadrotor helicopter," *IFAC Proc. Volumes*, vol. 41, no. 2, pp. 6513–6518, 2008.

[44] M. Morawiec, P. Strankowski, A. Lewicki, J. Guzinski, and F. Wilczynski, "Feedback control of multiphase induction machines with backstepping technique," *IEEE Trans. Ind. Electron.*, vol. 67, no. 6, pp. 4305–4314, Jun. 2020.

[45] G. Li and A. Khajepour, "Robust control of a hydraulically driven flexible arm using backstepping technique," *J. Sound Vib.*, vol. 280, nos. 3–5, pp. 759–775, Feb. 2005.

[46] J. Zhou, C. Wen, and G. Yang, "Adaptive backstepping stabilization of nonlinear uncertain systems with quantized input signal," *IEEE Trans. Autom. Control*, vol. 59, no. 2, pp. 460–464, Feb. 2014.

[47] D. Swaroop, J. K. Hedrick, P. P. Yip, and J. C. Gerdes, "Dynamic surface control for a class of nonlinear systems," *IEEE Trans. Autom. Control*, vol. 45, no. 10, pp. 1893–1899, Oct. 2000.

[48] Q. Shen and P. Shi, "Distributed command filtered backstepping consensus tracking control of nonlinear multiple-agent systems in strict-feedback form," *Automatica*, vol. 53, pp. 120–124, Mar. 2015.

[49] F. Wang, Z. Liu, Y. Zhang, X. Chen, and C. L. P. Chen, "Adaptive fuzzy dynamic surface control for a class of nonlinear systems with fuzzy dead zone and dynamic uncertainties," *Nonlinear Dyn.*, vol. 79, no. 3, pp. 1693–1709, Feb. 2015.

[50] A. T. Nguyen, N. Xuan-Mung, and S.-K. Hong, "Quadcopter adaptive trajectory tracking control: A new approach via backstepping technique," *Appl. Sci.*, vol. 9, no. 18, p. 3873, Sep. 2019.

[51] W. Zou, C. K. Ahn, and Z. Xiang, "Analysis on existence of compact set in neural network control for nonlinear systems," *Automatica*, vol. 120, Oct. 2020, Art. no. 109155.

[52] X. Wei and L. Guo, "Composite disturbance-observer-based control and $H_\infty$ control for complex continuous models," *Int. J. Robust Nonlinear Control*, vol. 20, no. 1, pp. 106–118, Jan. 2010.

**FEIYU JIN** is currently pursuing the master's degree with the School of Aircraft Engineering, Nanchang Hangkong University. His research interest includes cooperative control of multi-agent systems.

**LONGSHENG CHEN** received the M.S. degree in control theory and engineering from the Nanjing University of Aeronautics and Astronautics, Nanjing, China, in 2009. He is currently pursuing the Ph.D. degree in control science and engineering with East China Jiaotong University, Nanchang, China. He is also an Associate Professor with the School of Aircraft Engineering, Nanchang Hangkong University, Nanchang. His research interests include nonlinear system control and application, intelligent control, and multi-agent system control.

**WEIZHEN SUN** received the B.S. degree in aircraft manufacturing engineering from Nanchang Hangkong University, Nanchang, in 2021, where he is currently pursuing the master's degree. His research interests include the biomechanical mechanisms in fish swimming and the study of machine learning methods applied to fluid mechanics.

**YUXIANG WANG** is currently pursuing the master's degree with the School of Aircraft Engineering, Nanchang Hangkong University. His research interest includes cooperative control of multi-agent systems.

• • •